

Diplomarbeit

**Role of the gluconeogenesis enzyme PCK2
in anchorage-independent growth of lung cancer cells**

eingereicht von

David Hashemian Nik

zur Erlangung des akademischen Grades

Doktor der gesamten Heilkunde

(Dr. med. univ.)

an der

Medizinischen Universität Graz

ausgeführt an der

Universitätsklinik für Innere Medizin

Klinische Abteilung für Pulmonologie

unter der Anleitung von Betreuer*innen

Dr.in med. univ. Katharina Leithner, PhD

Gabriele Agnes Blümel, BSc MSc

Graz, 18.01.2022

Eidesstattliche Erklärung

Ich erkläre ehrenwörtlich, dass ich die vorliegende Arbeit selbstständig und ohne fremde Hilfe verfasst habe, andere als die angegebenen Quellen nicht verwendet habe und die den benutzten Quellen wörtlich oder inhaltlich entnommenen Stellen als solche kenntlich gemacht habe.

Graz, am 18.01.2022

David Hashemian Nik eh.

Danksagung

Ich möchte mich an dieser Stelle bei all denen bedanken die mich zur erfolgreichen Absolvierung dieser Diplomarbeit so tatkräftig unterstützt haben. An erster Stelle gebührt mein Dank meiner Hauptbetreuerin Univ.-Ass. Priv.-Doz. Dr. med. univ. Katharina Leithner, PhD für all die Mühe und fachliche Expertise in dieser nicht immer leichten Krisenzeit, welche durch Höhen und Täler geprägt war. Zudem möchte ich mich auch herzlich bei meiner Zweitbetreuerin Gabriele Blümel (ehemals Gabriele Grasmann) sowie Alexandra Bertsch, M.Sc. bedanken, von denen ich unschätzbar viel aus dem Bereich der Grundlagenforschung lernen konnte. Weiters gilt mein Dank der Medizinischen Universität Graz, welche das Projekt finanziell im Rahmen eines Förderungsstipendiums unterstützt hat sowie beim FWF Wissenschaftsfond für die Förderung (Einzelprojekt P33508 an Katharina Leithner). Auch meinen Eltern möchte ich dafür danken, dass sie mir das Studium ermöglicht haben. Danke auch an meine Freunde in Graz, mit denen ich auf eine großartige und abwechslungsreiche Studienzeit zurückblicken kann.

Table of contents

Danksagung	1
Table of contents.....	2
Abbreviations.....	5
List of figures	7
List of tables	9
Zusammenfassung.....	10
Abstract	11
1 Introduction	12
1.1 Lung Cancer.....	12
1.1.1 Epidemiology and risk factors.....	12
1.1.2 Histology & Prognosis.....	12
1.2 Warburg effect.....	13
1.3 Gluconeogenesis and PCK	13
1.4 Metabolic environment of cancer cells	16
1.5 Gluconeogenesis and the role of PCK in cancers	17
1.6 Matrix-detachment during metastasis.....	20
1.7 Reactive oxygen species (ROS)	21
2 Aims of this study	22
3 Methods & materials	23
3.1 Cell lines.....	23
3.2 Cell culture	23
3.3 Experimental media preparation	24
3.4 Buffers and reagents.....	25

3.5	Antibodies	26
3.6	Short-interfering ribonucleic acid (siRNA)	26
3.7	qPCR primers.....	28
3.8	Automated cell counting	28
3.9	Fluorescent-activating cell sorting analysis (FACS)	28
3.10	SDS-PAGE gel electrophoresis and Western blot	29
3.10.1	Sample preparation	29
3.10.2	BCA protein assay.....	29
3.10.3	SDS-PAGE electrophoresis and Western blot.....	29
3.11	Quantitative polymerase chain reaction (qPCR)	30
3.12	Establishment of cell viability measurements under detached conditions 31	
3.13	Transfection	31
3.14	Cell viability and viable cell number in growth conditions under matrix- independent environment and PCK2 silencing	32
3.15	Proliferation under matrix-independent growth conditions	32
3.16	PCK2 expression of H23 cells under adherent and matrix-detached growth conditions.....	34
3.17	Statistics.....	35
4	Results	36
4.1	Effect of growth media differences on matrix-independent cell viability and viable cell number	36
4.2	PCK2 expression in matrix-attached vs matrix-detached state	38
4.2.1	PCK2 protein expression	38
4.2.2	PCK2 RNA expression	39

4.3	Confirmation of PCK2 silencing on mRNA level.....	40
4.4	PCK2-silencing effects on viability and viable cell number.....	41
4.5	Proliferation assay.....	46
4.6	Gene expression analysis	48
4.6.1	Fatty acid synthase (FASN).....	48
4.6.2	GLUT-1 (SLC2A1)	49
4.6.3	Glutathione reductase (GSR).....	50
4.6.4	Thioredoxin reductase 1 (TXNRD1).....	51
5	Discussion.....	52
5.1	Interpretation of results.....	52
5.2	PCK2 demand due to raised FASN levels?.....	52
5.3	Serum may contain necessary growth and survival factors.....	53
5.4	Influence of glucose concentrations	53
5.5	Limitations	54
5.6	Outlook.....	54
5.7	Conclusion	55
6	References.....	56

Abbreviations

Acetyl-CoA	acetyl coenzyme A
AD	aqua destilata
ATP	Adenosine 5'-triphosphate
BSA	Bovine serum albumin
cAMP	3',5'-cyclic adenosine monophosphate
ccRCC	clear cell renal cell carcinoma
cDNA	Complementary desoxyribonucleic acid
CO ₂	carbon dioxide
Cp	Cycle threshold
CTC	circulating tumor cells
dFCS	dialyzed fetal calf serum
DMEM	Dulbecco's Modified Eagle Medium
ECM	extracellular matrix
ER	endoplasmatic reticulum
ERBB2	human epidermal growth factor receptor 2
FASN	fatty acid synthase
FBP 1	Fructose-1,6-bisphosphatase 1
FBP 2	Fructose-bisphosphatase 2
FCS	fetal calf serum
G6PC	Glucose-6-phosphatase
GGF	glucose-glutamine-free media
Gln	glutamine
Glu	glutamate
GPX4	gluthatione peroxidase 4
GSR	gluthatione reductase
GTP	Guanosine-5'-triphosphate
HCC	hepatocellular carcinoma
KRAS	Kirsten rat sarcoma viral oncogene homolog
MeOH	Methanol
MPE	malignant pleural effusion
NFAT	nuclear factor of activated T-cells
NSCLC	non-small cell lung cancer
OAA	oxaloacetate
PBS	Phosphate buffered saline
PC	pyruvate carboxylase
PCK	phosphoenolpyruvate carboxykinase
PDH	pyruvate dehydrogenase

PEP	phosphoenolpyruvate
PPP	pentose phosphate pathway
qPCR	quantitative polymerase chain reaction
RNA	ribonucleic acid
ROS	reactive oxygen species
RPMI	Roswell Park memorial institute
	sodium dodecylsulfate polyacrylamide gel
SDS-PAGE	electrophoresis
SLC2A1	gene for GLUT-1 glucose transporter
TBS	Tris-buffered saline
TBS-T	Tris-buffered saline with Tween20
TCA cycle	tricarboxylic acid cycle
TXNRD1	thioredoxin reductase
WHO	World Health Organisation
α -KG	α -ketoglutarate

List of figures

Figure 1: Overview of glycolysis, gluconeogenesis and branching biosynthetic pathways.	15
Figure 2: Glucose dependent metabolism in cancer cells.	19
Figure 3: Histogram of FACS analysis for the discrimination between living and dead cell fractions	36
Figure 4: Cell numbers and viability of H23 cells cultured in low attachment plates under various growth conditions.....	37
Figure 5: Western Blot of PCK2 expression in attached and detached A549 and H23 cells	39
Figure 6: PCK2 RNA expression in attached and detached A549 and H23 cells.	40
Figure 7: PCK2 expression analysis in H23 cells transfected with PCK2 siRNA and cultured in different growth media	41
Figure 8: Cell numbers and viability of matrix-detached H23 cells - 10 mM glucose and 10% dFCS.....	42
Figure 9: Cell numbers and viability of matrix-detached H23 cells - 1 mM glucose and 10% dFCS.....	43
Figure 10: Cell numbers and viability of matrix-detached H23 cells - 10 mM glucose and 0% dFCS	44
Figure 11: Cell numbers and viability of matrix-detached H23 cells - 1 mM glucose and 0% dFCS	45
Figure 12: Quality control of proliferation assay	46
Figure 13: Effect of different media on proliferation in detached H23 cells transfected with control siRNA (csi)	47
Figure 14: Effect of PCK2 silencing on proliferation in detached H23 cells in different media	48

Figure 15: Fatty acid synthase (FASN) RNA expression in attached and detached A549 and H23 cells analyzed using qPCR..... 49

Figure 16: SLC2A1 mRNA expression in attached and detached A549 and H23 cells analyzed using qPCR..... 50

Figure 17: GSR mRNA expression in attached and detached A549 and H23 cells analyzed using qPCR..... 50

Figure 18: TXNRD1 mRNA expression in attached and detached H23 and A549 cells analyzed by qPCR. 51

List of tables

Table 1: Growth media conditions	24
Table 2: Antibodies used	26
Table 3: siRNAs	27
Table 4: qPCR primer sequences	28

Zusammenfassung

Das Gluconeogeneseenzym Phosphoenolpyruvat Carboxykinase 2 (PCK2) kam kürzlich in den Fokus metabolomischer Studien und könnte die Tür zu neuen Antitumorstrategien öffnen. Vorherige Studien haben vielversprechende Effekte des PCK2 silencing bei adhärennten nicht-kleinzelligen Lungenkarzinom (NSCLC) Zellen unter niedrigen Glukosebedingungen aufgezeigt. Ziel unserer Studie war es ein geeignetes Experimentalmodell zu finden, um PCK2 Effekte unter extrazellulärer Matrixunabhängigkeit untersuchen zu können. Diese extrazelluläre Matrixunabhängigkeit ist unabdingbar für den Prozess der Metastasierung, bei der Zellen sich aus dem Zellverband lösen. Wir kultivierten H23 NSCLC Zellen unter glukosearmen und glukosereichen Bedingungen in speziellen ultra-low attachment Platten, mit und ohne Beigabe von Serum. Die Auswertung erfolgte mit Durchflusszytometrie, automatischer Zellzählung und Proliferationsmessungen. Zudem haben wir PCK2 Expression zwischen adhärennten und detached Zellen mittels Western Blot verglichen. PCK2 wurde in allen Bedingungen sowohl in adhärennten als auch nicht-adhärennten Zellen exprimiert, zwischen den Gruppen gab es keine signifikanten Unterschiede. PCK2 silencing mittels siRNA reduzierte die Lebendzellzahl signifikant sowohl in glukosereicher Kultur mit Serum ($p = 0.0031$ und $p = 0.041$) als auch in glukosearmer Kultur ohne Serum ($p = 0.0045$). Unter matrixunabhängigen Bedingungen führte vor allem das Fehlen von Serum zu einer signifikanten Reduktion der Lebendzellzahl und Proliferation. Es sind weitere Versuche erforderlich, um die Rolle von PCK2 auf Tumorzellüberleben unter matrixunabhängigen Bedingungen besser zu verstehen. Zusammenfassend konnten wir ein geeignetes Modell etablieren, welches es erlaubt, PCK2 Effekte auf Tumorzellüberleben unter verschiedenen matrixunabhängigen Bedingungen zu testen.

Abstract

The gluconeogenesis enzyme phosphoenolpyruvate carboxykinase 2 (PCK2) recently shifted into focus of metabolomic studies, possibly opening the door to new anti-tumor strategies. Previous studies have shown promising effects of PCK2 silencing in attached non-small cell like cancer (NSCLC) cells under low glucose environments. The main objective of this study was to establish a suitable experimental model to investigate the effect of PCK2 under the special circumstance of detachment from the extracellular matrix (ECM). ECM detachment is crucial in the formation of metastasis when tumor cells break free from their surrounding tissue. In our setting, H23 NSCLC PCK2 expressing or silenced cells were cultured in ultra-low attachment plates under high and low glucose conditions, with or without serum supplementation. As methods, we used fluorescent cell scanning analysis (FACS), automated cell counting (ACC) and proliferation assay. We also compared PCK2 expression differences between attached and detached cells using Western Blot. PCK2 was expressed in H23 cells under all conditions, no significant differences were found. PCK2 silencing by two pools of siRNAs significantly reduced viable cell number in high glucose, serum containing media ($p = 0.0031$ and $p = 0.041$) and low glucose, serum free media ($p = 0.0045$). Overall, the absence of serum led to a clear reduction in viable cell number and proliferation in non-adherent cells. An increased expression of fatty acid synthase under serum-free conditions suggests that the cells might lack serum lipids under these conditions. In conclusion, we found a suitable model to test PCK2 effects on cell survival in anchorage-independent growth conditions. The results suggest that PCK2 might play a role in growth of cancer cells under these conditions, however further studies are needed to clarify whether inhibition of PCK2 in tumors could potentially interfere with metastasis formation.

1 Introduction

1.1 Lung Cancer

1.1.1 Epidemiology and risk factors

About a century ago Adler I. described “that the primary malignant neoplasm of the lung is among the rarest of diseases” (1). Contradicting this statement, recent epidemiologic data from the World Health Organization (WHO) reported that in 2020 about 2.2 million new lung cancer cases have globally emerged (2). This accounts for 11.4% of all cancer types. The WHO also reported that in 2020 lung cancers had a mortality of over 1.7 million people making it the deadliest among all cancer types in most countries.

Main risk factor in the carcinogenesis of lung tumors is tobacco smoking, which has been studied since the 1950s (3). A 50-year cohort-study on almost 35.000 British male doctors compared the excess risk of acquiring lung cancer between continuous smokers and non-smokers (4). The result was a 20- to 50-fold risk increase. Cigarette smoke contains more than 60 carcinogens, some of them being tobacco-specific nitrosamines, polycyclic aromatic hydrocarbons, and aromatic amines (5). Although other risk factors, like viral, hormonal, or even genetics could have a role in carcinogenesis, the relative high incidence in non-smokers cannot be explained by dominant stand-out risk factors (6).

1.1.2 Histology & Prognosis

In general, lung cancers are either of small cell lung cancer type or part of the non-small cell lung cancer (NSCLC) group (7). NSCLC makes up about 85% of all lung cancer cases (8). Some of the more common lung cancer types of the NSCLC group found in biopsies and specimens are squamous cell carcinomas, adenocarcinomas and large cell carcinomas. Adenocarcinomas make up 42% of all lung cancers.

Most NSCLC patients are diagnosed at an advanced stage. Despite new advances in treatment of these patients, the 5-year survival rate remains poor at about 15%

when looked at all cancer stages together (9). Most deaths in lung cancer patients occur due to complications associated with metastasis, making it important to research new treatment strategies to prevent cancer spread.

1.2 Warburg effect

Since the 1920s, through the pioneering groundwork of Otto Warburg, it has been known that tumor cells prefer using glycolysis compared to normal tissue even when oxygen is abundant (10). This phenomenon is since referred to as the Warburg effect or aerobic glycolysis. Glycolysis describes the route in which glucose, the main energy source of most cells, through a series of enzymatic steps gets converted down into pyruvate. Then pyruvate usually can be converted into acetyl-CoA via pyruvate dehydrogenase (PDH) for further oxygen-dependent ATP engenderment in the mitochondria.

Aerobic glycolysis provides less energy in form of ATP per unit of glucose when compared with mitochondrial respiration. Interestingly, the metabolic rate of aerobic glycolysis is 10-100 times faster than the complete oxidation of glucose, resulting in comparable ATP production rates (11). One evolutionary-style theory suggests that this could have a survival advantage for tumor cells when competing for resources, especially when nutrients are scarce (12). Another advantage is that glycolysis produces metabolic intermediates that can be used to fuel biosynthetic pathways, allowing for biomass formation under uncontrolled proliferation (13).

1.3 Gluconeogenesis and PCK

Gluconeogenesis describes the endogenous anabolic synthesis of glucose, from non-sugar substrates. Within the human body, synthesis of new glucose mainly occurs in the liver and to a smaller degree in kidneys and intestine. Provision of glucose is crucial for glucose-dependent organs like the brain or erythrocytes, especially during fasting intervals. In the cell, synthesis of glucose takes place in the mitochondria, the cytosol and the endoplasmic reticulum (ER).

According to the literature, the first step of gluconeogenesis begins with the reaction of pyruvate into oxaloacetate (OAA) through the enzyme pyruvate carboxylase (PC) (14). Lactate and alanine can both be directly converted to pyruvate as entry point into gluconeogenesis. Glutamine and gluconeogenic amino acids are able to enter the Krebs cycle and get transformed into OAA. Further upstream, glycerol and serine can also be used as glycolytic or gluconeogenic intermediates.

Gluconeogenesis is tightly controlled by allosteric and hormonal regulators. This is of importance since reactions should only go in one way or the other and the rate of reactions should be limited. Acetyl-CoA, cAMP and the hormone glucagon are activators of gluconeogenesis (14). Insulin suppresses gluconeogenesis and stimulates glycolysis. Stress can also induce gluconeogenesis through epinephrine-mediated increased cAMP levels.

Biochemically gluconeogenesis is similar to the reverse pathway of glycolysis. However, some reactions are irreversible and require specific enzymes (**Figure 1**). One key enzyme of the gluconeogenic pathway is phosphoenolpyruvate carboxykinase (PCK or PEPCK) which catalyzes the reaction of oxaloacetate (OAA) and GTP into phosphoenolpyruvate, GDP and carbon dioxide (CO₂).

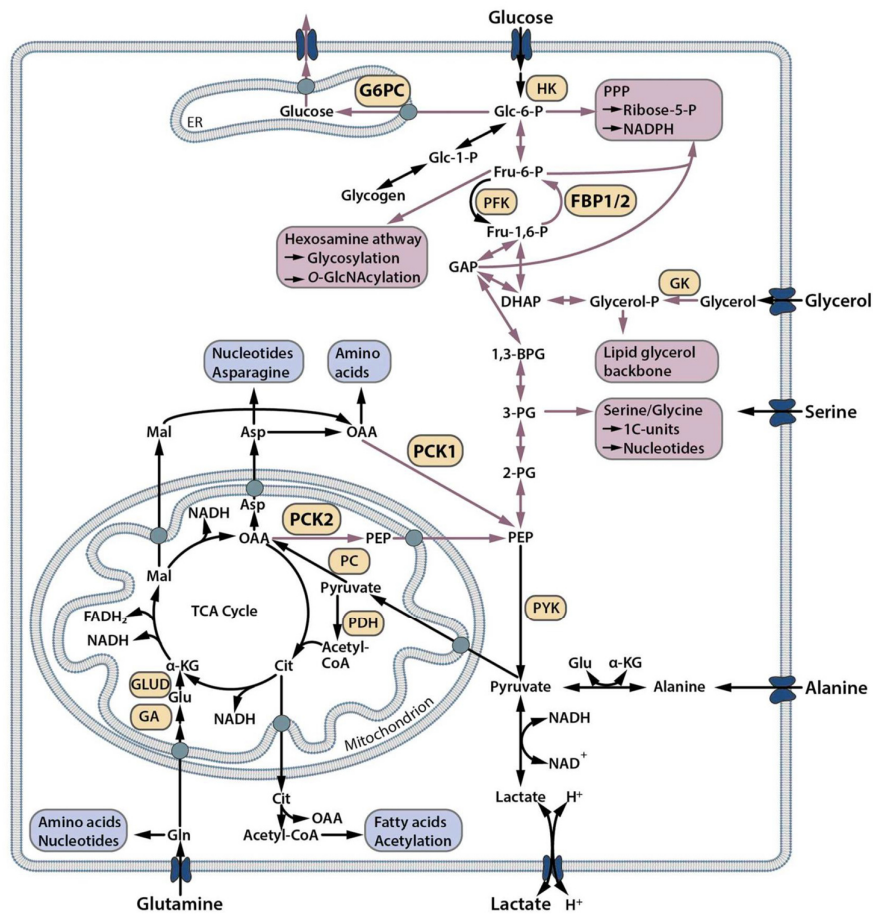


Figure 1: Overview of glycolysis, gluconeogenesis and branching biosynthetic pathways. Glycolysis aims to metabolize glucose step by step into pyruvate, which then can be shuttled into the citric acid cycle (TCA cycle, citric cycle, Krebs cycle) for further oxidative phosphorylation or get reduced to lactate. Gluconeogenesis (shown in red arrows) partly uses the same enzymes as glycolysis, with the exception of the key enzymes PCK, FBP1/2, and G6PC. Glycolytic/Gluconeogenic intermediates can be used as building blocks for biosynthetic pathways. Figure is reproduced from Grasmann et al., BBA - Reviews on Cancer, 2019, 2021 (15). Please visit the following websites for permission statements: [Rightslink® by Copyright Clearance Center Creative Commons — Attribution-NonCommercial-NoDerivatives 4.0 International — CC BY-NC-ND 4.0](#)

PCK exists in two variants, PCK1 (or PEPCK-C) the cytosolic isoform and PCK2 (or PEPCK-M) the mitochondrial isoform. It has been found that in the most common laboratory animals, the rat and the mouse, 90 to 95% of activity is PCK1, while in

most other mammalian species, including humans, both isoforms show about equal activity (16). Next to its metabolic role in gluconeogenesis PCK also acts in *glyceroneogenesis*, an abbreviated form of gluconeogenesis, by providing glycerol-3 phosphate for re-esterification of fatty acids into triglycerides (17). Additionally, PEPCK functions in a process called *cataplerosis*, meaning, the removal of TCA cycle anions generated from degraded amino acids. The cataplerotic function of PEPCK is especially relevant in glutamine metabolism in organs like the kidney cortex, in order to balance acid/base alterations and in the small intestine, where glutamine is metabolized to carbon dioxide (18).

1.4 Metabolic environment of cancer cells

As tumors grow, a process called angiogenesis occurs, resulting in new formation of vessels from pre-existing vasculature. The pre-mature vascular architecture is less efficient in delivering oxygen and nutrients, due to aberrant and leaky vessels (19). Tumor cells have to endure in microenvironments, defined by gradients of oxygen depletion, glucose deprivation, lactate, and pH in the extracellular space (20). Correspondingly, glucose levels in the interstitial fluid of tumors were measured to be lower than in plasma (21). Further, tumors inhabit low glucose environments, for example when lung cancer cells metastasize into the pleural space, causing malignant pleural effusion (MPE). Glucose levels, as low as 31 mg/dL or 1.7 mM, have been reported in sets of MPE samples (22). To endure under these cell-starving conditions, cells are able to use lactate, formerly thought to be only a waste product, as alternative fuel source (23). Lactate also fulfills the need as glucogenic precursor. In NSCLC cells the study group around Leithner et. al found that PCK2 plays a role in the conversion of lactate to the upstream phosphoenolpyruvate (PEP) under low glucose conditions (24). When glucose was abundant, NSCLC rather showed positive lactate production.

Amino acids present another group that can potentially fuel the metabolic need for cancer cell growth (25)(26). In proliferating and cancerous cells originating from mammalian tissue, amino acids were responsible for the majority of cell mass, even

when high amounts of glucose were utilized by cells (27). After the cell takes up an amino acid, the subsequent fate of conversion depends on the type of amino acid. Ketogenic amino acids get converted into acetyl-CoA, which can be condensed with OAA and enter the TCA cycle (citric acid cycle, Krebs cycle), but acetyl-CoA does not contribute net carbons to glucose, since for two carbons added by acetyl-CoA, two are lost as CO₂. Glucogenic amino acids, on the other hand, can add to glucose and thus to cell biomass, by branching from the TCA cycle as anabolic intermediates (28). The most prominent and widely available glucogenic amino acid in plasma is glutamine. Glutamine gets converted first intracellularly into glutamate and then α -ketoglutarate to enter the TCA cycle as anabolic precursor. Cancer cultured in-vitro often expressed glutamine dependency when cultured in standard tissue media. However, in human NSCLC and mouse KRAS-driven NSCLC, TCA cycle anaplerosis was found to be more dependent on glucose rather than glutamine (29–31). Bovine serum more closely resembles the environment of human blood. Interestingly, A549, a NSCLC cell line, cultured with bovine serum, exhibited less dependency on glutamine, for TCA cycle anaplerosis (32). This suggests that tumors in-vivo probably exhibit similar independency of glutamine metabolism.

1.5 Gluconeogenesis and the role of PCK in cancers

Tumors deriving from gluconeogenic tissues, like e.g., hepatocellular carcinoma (HCC) and clear cell renal cell carcinoma (ccRCC), express lower amounts of PCK1 or PCK2 compared to normal liver tissue (33). In line gene analysis of ccRCC patients showed significant under-expression of the PCK1 gene (34). In these gluconeogenic tumors, PCK acts as a tumor suppressor because it counteracts glycolysis and the TCA cycle, thereby affecting energy homeostasis. However, the function of PCK1 in HCC was questioned in a study, finding that PCK1 also acts as activator of the sterol regulatory element-binding protein and therefore supports tumor proliferation (35).

Some cancers have been shown to express PCK to maintain gluconeogenesis, in order to fulfill biosynthetic requirements under nutrient-poor environments (**Figure**

2). This process was first depicted in lung cancer cells under glucose deprivation, where PCK2 was upregulated and isotopically labelled lactate was converted into phosphoenolpyruvate in a PCK2-dependent manner (24). Tissue analysis confirmed that PCK2 in fact is generally overexpressed in cancerous NSCLC tissue compared to normal lung tissue (36). Investigations done by our study group in silencing experiments with siRNAs targeting PCK2, have shown decreased cell growth and induced apoptosis in A549 and H23 NSCLC cells under low glucose environments, as well as reduced growth in 3D spheroid models (24). This gives evidence that some NSCLC cell lines depend on PCK2 to some extent to survive under tough metabolic conditions. PCK1 and PCK2 might enable cancer cells, even when there is no glucose available, to produce precursors for important biomolecules, the phospholipid glycerol backbone (37), serine and glycine (38) (39) which are necessary for purine synthesis, and ribose phosphate (40) (41) through the pentose phosphate way.

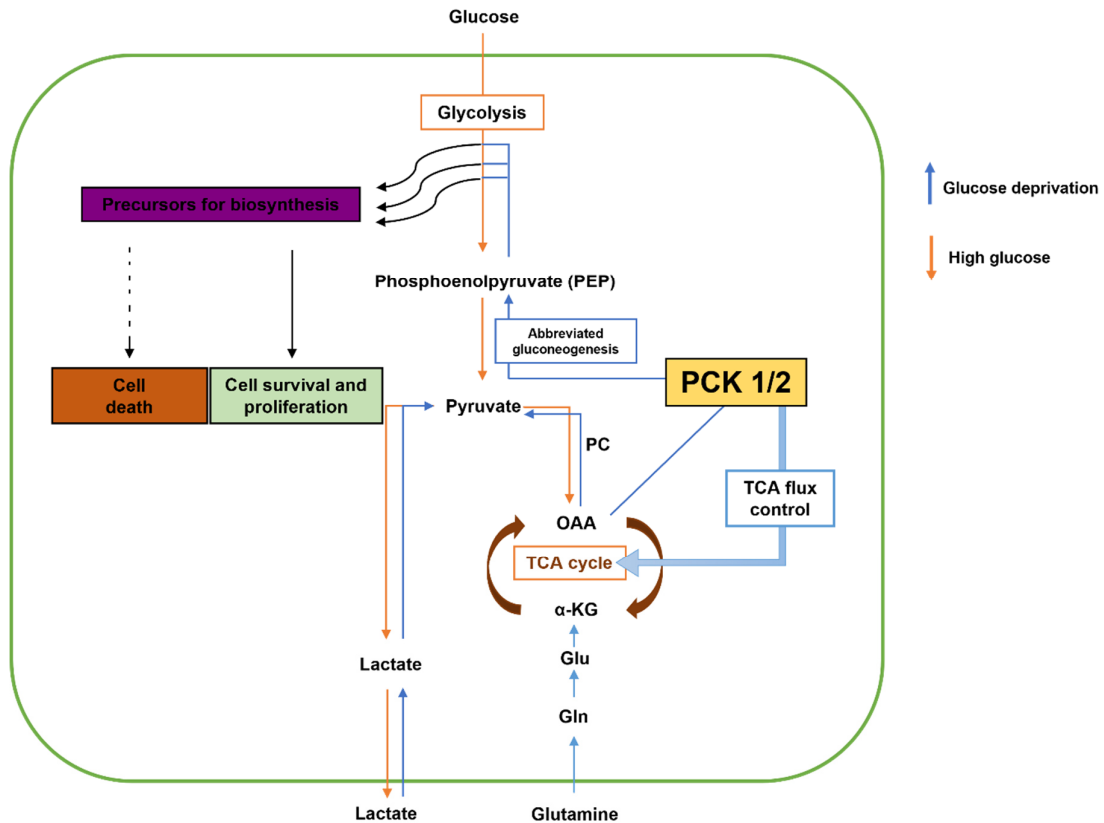


Figure 2: Glucose dependent metabolism in cancer cells. Depending on the environment, cancer cells must adapt to various glucose conditions. PCK1/2 engages in abbreviated gluconeogenesis to create biosynthetic precursors that ultimately are essential for cell survival and proliferation. The influence of PCK1/2 on TCA cycle flux can feed more glutamine into anaplerosis to create OAA. TCA, tricarboxylic cycle; PCK1/2, phosphoenolpyruvate carboxykinase 1/2; OAA, oxaloacetate; Glu, glutamate; Gln, glutamine; α-KG, α-ketoglutarate.

Glutamine acts as important contributor to the TCA cycle in cancer, despite glucose availability, as described in a review in 2016 by DeBerardinis et. al. (28) and outlined above. PEPCK knockout was found to be associated with reduced abundance of the TCA cycle intermediates citrate, malate and α-ketoglutarate in ¹³C-glucose labeled cells (42). Recently, PCK2 was shown to mediate cataplerosis and the synthesis of glutamine derived gluconeogenic intermediates in glucose and serum starved lung cancer cells (43). The generation of PEP through PCK2 was shown to be occurring even when glucose was present in colon carcinoma cells (44). It was

suggested that the PEPCK pathway, through PEP as metabolic second messenger, regulated the nuclear factor of activated T-cells (NFAT) and MYC signaling pathways through the PEP/Ca²⁺ axis.

1.6 Matrix-detachment during metastasis

The ability to metastasize is one of the hallmarks of cancer cells and is necessary for spread into other tissues and organs. Cells need the ability to detach from their tissue and survive to some extent without attachment to the extracellular matrix (ECM) when circulating to a new metastatic site. Usually, when cells lose anchorage to their surroundings, they undergo a programmed cell death program called anoikis (45). This mechanism is of physiological importance to prevent unwanted migration to a new site, however some cells can physiologically detach from their surrounding in order to migrate, when necessary, like e.g. in keratinocyte migration during the wound healing process as reaction to a skin lesion.

Cancer cells develop their own strategies to avoid anoikis for metastasis. When adhesion to the ECM is lost, cells utilize a phenotype of forming circulating tumor cell clusters (CTC clusters), which can increase the metastatic potential (46). The exact mechanism remains unknown. For epithelial cells it has been shown that ECM detachment induces autophagy, the degradation of cellular components, which in turn promoted cell survival during anoikis (47). Autophagy can also help cells to recycle nutrients under starvation conditions (48).

Matrix detached cells have been shown to have reduced glucose uptake, which can be rescued through overexpression of oncogenes, like e.g. human epidermal growth factor receptor 2 (ERBB2) in mammary epithelial cells (49). Reduced glucose uptake, potentially poses a metabolic challenge for tumor cells that usually require large amounts of substrates for rapid growth. In the same study, matrix-detachment induced a significant increase in reactive oxygen species (ROS).

Another distinct form of cell death than can occur under matrix detachment is ferroptosis (50). Ferroptosis is characterized by failure of glutathione peroxidase 4

(GPX4) which tries to reduce lipid peroxides. Ferroptosis is known to be inhibited when cells show certain integrin signaling phenotypes (51).

1.7 Reactive oxygen species (ROS)

The group of ROS are molecules derived from O₂ that have a high affinity to react with other molecules. The right balance of ROS production and ROS disposal determines whether ROS have harmful or protective effects on the cell's health. ROS can be generated by cellular respiration, as metabolic byproducts, by enzymatic synthesis and physical or chemical factors (52). To counter increased stress, cells have defense mechanisms to eliminate ROS. Some enzymatic defenses present are superoxide dismutases, thioredoxin, the glutathione pathway, catalase, peroxiredoxins and mitochondrial K⁺ channels (52). Additionally, antioxidant scavenger molecules like tocopherol (Vit E), ascorbic acid (Vit C), carotenoids, uric acid and polyphenols can relieve ROS induced stress (52).

During ECM detachment, ROS levels have been shown to be increased, while reduced glutathione was decreased (49). Just like glucose uptake impairment, ROS levels were rescued when cells expressed ERBB2 (49). ROS level increase preceded the reduced glucose uptake. It was suggested that this was due to a reduced glycolytic flux affecting the pentose phosphate pathway (PPP). The PPP can increase resistance to oxidative stress, thanks to oxidative branches and NADPH production (53). During ECM detachment, PCK2 could in theory support the cells guard against ROS levels under glucose deprivation or reduced glycolysis by fueling the gluconeogenesis pathway for the PPP.

2 Aims of this study

Precedent works of our study group already suggested that NSCLC need PCK2 to maintain their metabolic activity through gluconeogenesis when subjected to nutrient poor environments (24). Cells that detach from the ECM are of special interest, since they represent an important step in cancer progression, metastatic spread. The specific role of PCK2 and gluconeogenesis in matrix-detached cancer cells is unknown. In this study we aimed to test the influence of PCK2 in matrix detached NSCLC cells under different metabolic conditions on cell survival and proliferation. Following literature, we used high and low glucose treatments, according to the possible range of glucose levels *in vivo*. Moreover, we examined the impact of matrix detachment and nutrient scarcity on PCK2 expression and other possibly affected metabolic genes. The results of this study could bring new insights into the metabolic rewiring in matrix detached NSCLC cells facing nutrient deprivation.

3 Methods & materials

3.1 Cell lines

In this study two different human NSCLC lines have been used. One cell line is NCI-H23 (ATCC number CRL-5800) obtained from the American Type Culture Collection (ATCC, Manassas, VA). The other cell line is A549 (Cat. No. 300114) obtained from Cell Lines Service (Eppelheim, Germany). For simplicity, these cell lines are further referred to as H23 and A549.

3.2 Cell culture

H23 and A549 cells were cultivated at 37°C under 5% CO₂ and 98% humidity. Culture medium for A549 was Dulbecco's Modified Eagle Medium: Nutrient Mixture F12 (DMEM/F12) 1:1 (Gibco, Carlsbad, CA) supplemented with 10 % fetal bovine serum (FCS) (Biowest, France), L-glutamine (Gibco), 100 U/mL penicillin and 100 µg/mL streptomycin. Culture medium for H23 was Roswell Park memorial institute (RPMI) 1640 (Gibco) supplemented with 10% FCS (Biowest, France), L-glutamine (Gibco) 100 U/ml penicillin and 100 µg/mL streptomycin. Above mentioned media are further referred to as DMEM/F12 complete and RPMI 1640 complete. Cells were splitted twice per week and media was changed in between. Under our culturing conditions, A549 were doubling once per day and H23 cells were doubling every 2-3 days. Cells were washed briefly with phosphate buffered saline pH 7.4 (PBS). Cells were detached from the cultivating flask using Trypsin/EDTA (Gibco Thermo Fisher, cat. no. 25300054). Trypsin reaction was stopped with DMEM/F12 complete for A549 and RPMI 1640 complete for H23. The suspension was then centrifuged at 400 G for 5 minutes and supernatant was removed. Cells then received fresh complete media and were cultivated in 75 cm² cultivating flasks.

3.3 Experimental media preparation

We created four different media, simulating various environments of glucose and serum conditions. Cells were treated with glucose-glutamine-free media of DMEM or RPMI (DMEM-GGF/ RPMI-GGF). DMEM-GGF was purchased from Gibco, Thermo fisher scientific, cat. no. A422563. RPMI-GGF was prepared from glucose, glutamine, arginine, and lysine-free RPMI SILAC (A2494201, Gibco) supplemented with 1.15 mM arginine and 0.27 mM lysine. GGF media were supplemented with 100 U/mL penicillin, and 100 µg/mL streptomycin. Media either contained 10 % dialyzed fetal bovine serum (dFCS) or no dFCS. Additionally, media were supplemented with stocks of 1000 mM glucose and 200 mM glutamine to create two different glucose concentration as shown in **Table 1**, and a final glutamine concentration of 2 mM. Glucose and glutamine stocks were diluted in aqua dest., sterile filtered through 0.22 µm filters, and stored at -20°C. Due to their specific media preference, A549 cells were treated with DMEM-based media, while H23 received RPMI-based media.

Table 1: Growth media conditions

Serum-containing media	Glucose	Glutamine	dFCS
1 mM Glc 10% dFCS	1 mM	2 mM	10%
10 mM Glc 10% dFCS	10 mM	2 mM	10%
Serum-free media	Glucose	Glutamine	dFCS
1 mM Glc 0% dFCS	1 mM	2 mM	0%
10 mM Glc 0% dFCS	10 mM	2 mM	0%

3.4 Buffers and reagents

- 5 x Laemmli buffer
- 10x TBS: 31.5 g Tris HCl, 80 g NaCl to 1L with A. dest. (AD) Adjusted to pH of 7,5 with 10 M NaOH
- TBST: 200 mL 10x TBS, 1800 mL AD, 2000 μ L Tween 20
- MTBST: 5 g milk powder, 100 mL TBST
- 10x Running Buffer: 30 g Tris Base, 144 g Glycine, 100 mL 10% SDS to 1 L with AD
- 1x Running Buffer: 100 mL 10x Running Buffer to 1 L with AD.
- 10x transfer buffer: 56 g Trizma Base, 286 g Glycine, to 2 L with AD
- 5% BSA: 5 g BSA, 100 mL TBST
- 5% milk solution: 5 g milk powder, 100 mL TBST
- 1x transfer buffer: 200 mL 10x transfer buffer, 1400 mL AD, 400 mL Methanol (MeOH)
- 10% APS: 1 g Ammonium persulphate, 10 mL AD (Millipore), Aliquots stored at -20°C
- 5x Sample buffer: 300 μ L Tris HCl pH 6.8, 2mL SDS 10%, 1 mL glycerol, 500 μ L beta-mercaptoethanol, to 10 mL with AD, add 1 mg bromphenol blue, aliquoted, stored at -20°C.
- TEMED: N,N,N',N'-tetra-methyl-ethylenediamine
- 10% SDS: Sodium dodecyl sulphate 10% w/v in AD

3.5 Antibodies

Table 2: Antibodies used

Primary antibody	Dilution	Catalogue No.	Manufacturer
Beta actin	1:3000	Sc-47778	Santa Cruz Biotechnology
PCK2	1:2000	ab187145	Abcam

Secondary antibody	Dilution	Catalogue No.	Manufacturer
Anti mouse-HRP	1:3000 – 1:5000	#7076	Cell Signaling
Anti rabbit-HRP	1:3000	#7074	Cell Signaling

Beta actin antibodies were diluted in 5% milk TBST, and membranes were blocked with 5% milk TBST (MTBST). PCK2 antibodies were diluted in 5% BSA TBST and membranes were blocked with 5% BSA TBST.

3.6 Short-interfering ribonucleic acid (siRNA)

Short-interfering RNAs (siRNAs) consist of two strands. One strand is the antisense, or guiding strand. The other strand is called the sense, or passenger strand. Both strands form a duplex ranging from 19 to 25 bp in length. siRNAs are designed to knock out a specific target-gene, by complementing ribonucleic acid molecules, thus impairing their function. Every siRNA experiment should include controls; therefore, we used non-targeting control siRNA (csi).

Table 3: siRNAs

Type	Name	Target sequence	Catalogue no.	Manufacturer
PCK2 siRNA #1 (pool of 4 siRNAs)	ON-TARGETplus Human PCK2 (5106) siRNA	GCAAGCAUGCGUAUUAUGA, GAGCAAGACGGUGAUUGUA, GAUUUGCUUGGAUGAGGU, CCUGGGAGAUGGUGACUUU	L-006797- 00-0005	Dharmacon
PCK2 siRNA #2 (pool of 2 siRNAs)	Custom siRNA, ON-TARGETplus	GGAUGAGGUUUGACAGUGAUU, UGGCUACAAUCCAGAGUAAUU	CTM- 509915, HR1ZN- 006815	Dharmacon
Control siRNA	ON-TARGETplus Non-targeting pool	UGGUUUACAUGUCGACUAA, UGGUUUACAUGUUGUGUGA, UGGUUUACAAUGUUUUCUGA, UGGUUUACAUGUUUUCCUA	D-001810- 10-05	Dharmacon

3.7 qPCR primers

Table 4: qPCR primer sequences

qPCR Primer	Manufacturer	Forward sequence/ reverse sequence
PCK2 (phosphoenolpyruvate carboxykinase 2)	Eurofins	F: 5'-CATCCGAAAGCTCCCCAAGTA-3' R: 5'-TGGAAATCAGCTGGGGACATC-3'
FASN (fatty acid synthase)	Eurofins	F: 5'-TCGTGTTGACTTCTCGCTCC-3' R: 5'-CCATCTCTCAAGACCACGGC-3'
SLC2A1 (Glucose transporter)	Eurofins	F: 5'-TGGCATCAACGCTGTCTTCT-3' R: 5'-AGCCAATGGTGGCATAACA-3'
GSR (glutathione reductase)	Eurofins	F: 5'-CAGCGTCATTGTTGGTGCAG-3' R: 5'-CCTTGACCTGGGAGAACTTCAG-3'
TXNRD1 (thioredoxin reductase)	Eurofins	F: 5'-CGATCTGCCCGTTGTGTTTG-3' R: 5'-TATTGGGCTGCCTCCTTAGC-3'

3.8 Automated cell counting

We used TC20™ Automated Cell Counter (Bio-Rad) to detect viable cell numbers. Dead cells accumulate trypan blue solution within their cytoplasm. The machine detects cell viability through multifocal plane analysis. Gate size was set between 5 and 20 nm. The detection range ranges from $5 \cdot 10^4$ to $1 \cdot 10^7$ cells/mL.

3.9 Fluorescent-activating cell sorting analysis (FACS)

In our experiments we used the fluorescent agent CellTrace™ Calcein Red-Orange (Thermo Fisher, cat. no. C34851) aliquoted and stored at -20°C. Living cells keep the fluorescent Calcein in their cytoplasm, while dead cells cannot. This method

allowed us to evaluate cell viability, defined as the fraction of living cells. Measurement occurred on the CytoFLEX (Beckman Coulter, Brea, California, USA).

3.10 SDS-PAGE gel electrophoresis and Western blot

We performed SDS-PAGE gel electrophoresis to separate cell proteins. Additionally, Western Blot was used to detect the amount of protein.

3.10.1 Sample preparation

Cells were washed with PBS and suspended in RIPA Buffer. For adherent cells, cells were washed once with PBS, then RIPA Buffer was directly added to the well and then cells were scraped and transferred to Eppendorf tubes. Cell lysates were homogenized using a sonicator (Ultraschall-Desintegrator UP50H ROTH, Carl Roth GmbH+Co.KG Karlsruhe, Germany) at amplitude 80 and cycle 1. Every probe was sonicated three times for five seconds. Excess compounds were removed through centrifugation at 13 000 rpm for 10 minutes at 4°C. The supernatants were stored at -20°C.

3.10.2 BCA protein assay

BCA (bicinchononic acid) Protein Assay kit (Thermo Scientific) was used to measure overall protein concentration. 25 µL of diluted sample (1:5) was mixed with 200 µL of BCA solution. A dilution chain of 2 mg/ml BSA stock was used to create a linear calibration curve. Absorption was measured at 562 nm in 96 well plates using the Spectramax Plus 384 (Molecular Devices, Orleans Drive Sunnyvale, CA).

3.10.3 SDS-PAGE electrophoresis and Western blot

For SDS- polyacrylamide gel electrophoresis (SDS-PAGE) we used 10% SDS-gels set in the Biorad Mini-PROTEAN® 3 cell (Biorad, USA). All buffers and reagents used are described in detail in **Section 3.4**. Samples were mixed 1:1 with Laemmli Buffer and incubated for 10 minutes at 95°C in thermomixer. For electrophoresis 50 µg of protein sample was loaded in each chamber and current was set to 180 Volts

for 90 minutes. Before transfer, the PDVF membrane (BioRad) was pre-activated for 15 seconds in MeOH. Transfer was run at 400 mA for 90 minutes. The membrane was blocked with MTBST or TBST containing 5% BSA for 1 hour at room temperature. Overnight incubation with the first antibody was performed at 4°C. After three-time washing with TBST for 10 minutes, the membrane received the second antibody and was incubated for 1 hour at room temperature. Again, the membrane was washed three times with TBST for 15 min. For chemiluminescent detection of protein, the immunodetection substrate (SuperSignal® West Pico chemiluminescent substrate, Thermo Scientific) was applied. The membrane was analyzed using the ChemiDoc Touch (BioRad).

Protein expression was quantified using Image Lab©. Intensity values were normalized to probes with high glucose and with serum, and then to beta-actin.

3.11 Quantitative polymerase chain reaction (qPCR)

RNA was extracted and purified from other nucleotide molecules using the peqGOLD Total RNA kit (VWR, Vienna, Austria) according to manufacturer's protocol and eluted RNA was stored at -70°C. RNA quantity was measured using NanoDrop (Thermo Scientific, Fremont, USA) to determine if enough RNA for measurement was present in samples. The extracted RNA was transcribed into cDNA using qScript cDNA Synthesis Kit (Quantana Biosciences). The reaction creating cDNA was performed in the MyCycler™ thermal cycler (Bio-Rad). Quantitative, real-time cDNA analysis was performed in the LightCycler 480 (Roche) using the Biozym Blue´SGreen qPCR Mix (Biozym) and primers listed in **Table 4**. For qPCR experiments, ΔC_p values were calculated by subtracting the C_p value of the gene of interest from the C_p value of the housekeeping gene 18S. For $\Delta\Delta C_p$, ΔC_p of the control siRNA group was subtracted from the ΔC_p of PCK2 siRNA groups. Finally, the n-fold gene expression was determined by calculating $2^{-\Delta\Delta C_p}$ formula.

3.12 Establishment of cell viability measurements under detached conditions

Automated cell counting (ACC) and FACS need a minimum threshold of cells to reach the detection range. Our first experiments started with 50 000 A549 and H23 cells, that were treated with serum-free and serum-containing media for 24, 48 and 72 hours in ultra-low attachment 24-well plates (VWR, cat. no. 734-1584). After 24, 48- and 72-hours ACC was performed. 72 hours after treatment FACS was performed.

3.13 Transfection

Transfection, describes the delivery mechanism, by which siRNAs are incorporated into cells. A variety of transfection methods have been established including transfection with cationic liposomes, electroporation, viral-mediated delivery and modified siRNAs. Each method comes with its own advantages and disadvantages. In transfection experiments we used Jet Prime® Kit (Polypus-Transfection, New York, USA), an established method in transfecting H23 cells.

H23 cells, counted with CASY® cell counter (Schärfe System, Reutlingen, Germany), were plated in 6-well plates (VWR, cat. no. 734-0019) at 200 000 cells per well. We incubated cells for 24 hours at 37°C, to allow adhesion to occur. Cells were transfected with siRNAs listed in

Table 3 using Jet Prime® kit according to the manufacturer's protocol. As control group, three wells were left non-transfected (NT). 24 hours after transfection, all cells received fresh RPMI complete medium.

3.14 Cell viability and viable cell number in growth conditions under matrix-independent environment and PCK2 silencing

48 hours after transfection with PCK2 siRNA, 50 000 cells were re-plated to separate wells of 24-well ultra-low attachment plates (VWR, cat. no. 734-1584). All main cell groups: NT, csi, PCK2 #1 and PCK2 #2 were distributed to 9 wells and each cell group received different media, listed in table **Table 1**. Treatment with serum-free and serum-containing media was limited to 24 hours.

After media treatment, non-adherent cells from 6 wells (300 000) were combined into 15 mL tubes and centrifuged at 400 G for 5 minutes. Cells were resuspended in 1 mL of PBS and again centrifuged at 400 G for 5 minutes. Calcein solution was prepared by diluting CellTrace™ Calcein Red-Orange 1:5000 in PBS. Cells were resuspended in Calcein solution and incubated for 20 minutes at 37°C. Then viability was measured between groups with FACS analysis described in **Section 3.9**.

To get a better picture, we also looked at viable cell numbers. To this end, we performed automated cell counting to evaluate differences in living cell counts. Non-adherent cells from 3 wells (150 000 cells) were combined after 24-hour treatment, briefly resuspended, and then transferred to 1.5 mL Eppendorf tubes. Cells were centrifuged at 400 G for 5 min and resuspended in 100 µL PBS. For measurement on the Automated Cell counter, 20 µL of suspension were combined with 20 µL of Trypan blue solution (Biorad) and placed on measurement cartridges. Leftovers were placed in 350 µL of RNA lysis buffer or 100 µL of Ripa Buffer solution.

3.15 Proliferation under matrix-independent growth conditions

H23 cells were transfected using two different pools of PCK2-siRNA (Dharmacon, Smartpool), control siRNA (Dharmacon Smart Pool) and Jet Prime® Kit as

described in **Section 3.13**. After transfection, 300 000 H23 cells were cultured in growth media for 24 hours using ultra-low attachment plates (VWR). For positive and negative control of attached cells, 200 000 transfected cells were cultured in normal 6-well plates nurtured by RPMI complete. An extra of 300 000 csi cells were cultured in medium 1 on ultra-low-attachment plates. These extra csi cells were used as negative control for detached cells. To assess proliferation, Click-iT™ EdU Cell Proliferation Kit for Imaging (Thermo Fisher Scientific) was used. EdU, chemically known as 5-ethyl-2'-deoxyuridine, is a thymidine analogue that is incorporated into newly synthesized DNA during active DNA synthesis. The reaction is made visible by attachment of a bright, photostable dye. The EdU 10 mM stock solution was diluted to 1 mM using RPMI 1640 SILAC (Gibco), supplemented with L-Arginine and L-Lysine. 5 µL of 1 mM EdU solution was pipetted in each well of detached condition to obtain a final EdU concentration of 10 µM. Cells were then incubated at 37°C and 98% humidity for 90 minutes. Cells were collected and centrifuged. Collected cells were resuspended in 1% BSA solution. Then Click-iT fixative (component D) was used to keep cells mildly fixed and allow for the EdU to gain access to the DNA. To make cells permeable for the dye reaction, click-iT saponin based permeabilization reagent was pipetted on cells before and after a 15-minute incubation time with click-IT reaction cocktail, containing copper sulfate, the fluorescent dye Alexa Fluor® 488 and buffer additive. Measurements took place on the CytoFLEX (Beckman Coulter, Brea, California, USA). All FACS analyses were performed using 488 nm for excitation and 530 nm for emission. For media differences, proliferation results of cells with control siRNA (csi) in different media were normalized to csi in 10 mM glucose and 10% dFCS. Transfections effects of PCK2 siRNA #1 & #2 on proliferation were normalized to control siRNA of the same media.

3.16 PCK2 expression of H23 cells under adherent and matrix-detached growth conditions

A549 and H23 cells were used in this experiment. Two groups, an adherent, and matrix-detached group, were cultured in different growth media, to be subsequently analyzed for differences in PCK2 protein and PCK2 RNA expression. Additionally, expression differences of FASN, SLC1A2, GSR and TXNRD1 were analyzed between the two groups.

For the adherent cell group, 150 000 cells per well were plated into conventional 6-well plates. We cultivated cells for 24 hours in DMEM/F12 complete and RPMI 1640 complete, for A549 and H23 respectively to allow adhesion to occur. Thereafter, cells were briefly washed twice with 2 mL PBS and treated with 2 mL of growth media. After 18 hours, media were removed from the cells and cells were washed once with PBS. Then 100 μ L RIPA Buffer was directly added to wells. A reduced duration of treatment compared to the cell viability assays was selected in order to limit cell death. Plates were scraped and the protein lysate was transferred on pre-cooled Eppendorf tubes and stored at -20°C .

For the matrix-detached group 300 000 cells were placed in 15 mL Eppendorf tubes and centrifuged with 6 mL PBS at 400 G for 5 minutes. Cells then were resuspended in 3 mL of growth media and 0.5 mL per well were distributed into ultra-low attachment 24-well plates. Like in the adherent group, 18 hours after treatment, the detached cells were harvested in two 1.5 mL Eppendorf tubes and centrifuged at 400G for 5 minutes. Next, cells were resuspended in 0.5 mL PBS and centrifuged again at 400 G for 5 minutes. Finally, cells were resuspended in 50 μ L RIPA buffer or in RNA lysis buffer and stored at -20°C . For Western blot, cell lysates of both adherent and matrix-detached cells were then prepared and analyzed for SDS-PAGE gel electrophoresis and Western Blot as described in **Section 3.10** with antibodies listed in **Table 2**. For RNA analysis, cells have been stored in RNA lysis buffer at -20°C until RNA extraction, cDNA synthesis and qPCR as described in

Section 3.11. RNA expression differences of PCK2, FASN, SLCA1, GSR, and TXNRD1 were analyzed between groups of the same cell line.

3.17 Statistics

All statistics were performed using Excel 2019 or SPSS software. For comparison either a two-sided, unpaired t-test or a one-group t-test was used as applicable. P-values below 0.05 were considered significant. Graphical illustrations were created in Excel 2019.

4 Results

4.1 Effect of growth media differences on matrix-independent cell viability and viable cell number

Main focus of this study was to investigate the role of PCK2 during ECM detachment under different starvation conditions. Our first focus was to see how cells would react when cultured in a matrix-independent setting under high or low glucose treatment, and with or without serum. As indicators of general cell survival, cell viability and the absolute viable cell number were measured. All results were compared to cells treated with high glucose and serum.

To confirm that FACS analysis, using the calcein dye, properly distinguished between living and dead cells, we included a negative control group of dead cells through treatment with ethanol. Histogram data showed a clear distinction between dead and living cells (**Figure 3**).

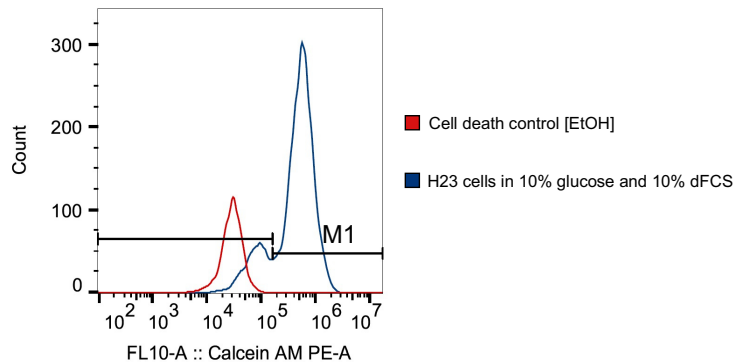


Figure 3: Histogram of FACS analysis for the discrimination between living and dead cell fractions. As a negative control (cell death control), cells were treated for 10 minutes with 70% ethanol (EtOH). For positive control (viable cells), non-transfected H23 cells were cultivated in 10 mM glucose and 10% dFCS. Viable cells show a positive calcein AM fluorescence (M1).

Matrix-independent H23 cells cultured in serum-free media, showed a significant reduction in cell viability and viable cell number (**Figure 4**). In FACS absorption

curves, a slight shift between peaks was observed between serum groups, so that gates were adapted for both conditions. Viable cell numbers decreased drastically, approximating that numbers plummeted to about a twentieth to that of cells treated with serum. In contrast, glucose concentration had no notable impact on cell survival. Morphologically, cells grouped together and formed multiple cell clusters, an expected feature during ECM detachment (**Figure 4, D**). In summary, serum-availability heavily affects viable cell number and viability in ECM detached H23 cells.

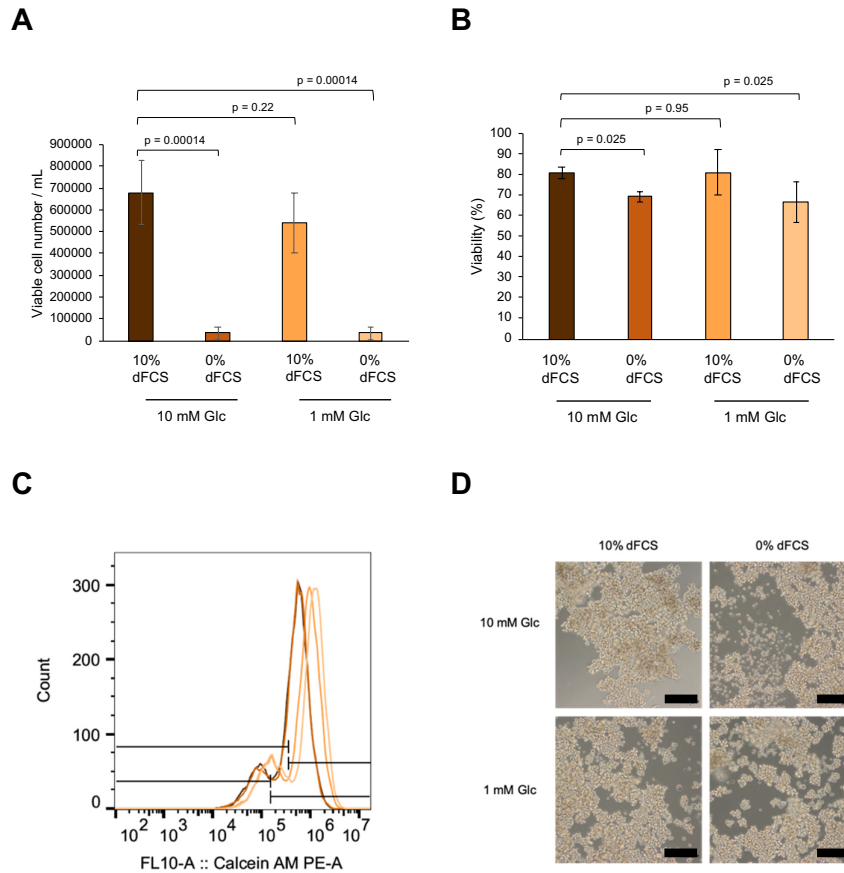


Figure 4: Cell numbers and viability of H23 cells cultured in low attachment plates under various growth conditions. Cells were plated in to low attachment plates in medium containing high or low glucose (Glc) concentrations with or without dialyzed fetal calf serum (dFCS) for 24 hours.

(A) Viable cell number was measured with the BioRad automated cell counter using Trypan Blue solution. (B) Cell viability was measured with FACS. Calcein-AM was used as the detection reagent. (C) Representative overlay of FACS absorption curves of all different conditions media groups. The left peak represents the proportion of dead cells, the right peak the proportion of living cells. Dark brown = 10 mM glucose, 10 % dFCS, brown = 1 mM glucose, 10 % dFCS, orange = 10 mM glucose, 0 % dFCS, light orange = 1 mM glucose, 0 % dFCS. (D) Phase-contrast microscopy of detached H23 cells after 24 hours treatment time. Scale bar = 200 μ m. Data presented is mean \pm standard error of the mean (SEM) from four independent experiments.

4.2 PCK2 expression in matrix-attached vs matrix-detached state

4.2.1 PCK2 protein expression

To test the hypothesis that PCK2 expression might differ in cells that are matrix-detached vs. attached, we cultivated A549 and H23 cells in attached and detached growth environments for 18 hours. As loading control, beta-actin was used to check visually for regular protein banding and to normalize probes in later analysis.

Quantification of Western blots showed no significant expression differences between 1 and 10 mM glucose concentrations in detached cells treated with serum-containing media (**Figure 5**). Cells cultured under serum-free conditions could unfortunately not be tested for protein in this setting, due to insufficient protein quantities measured in BCA analysis.

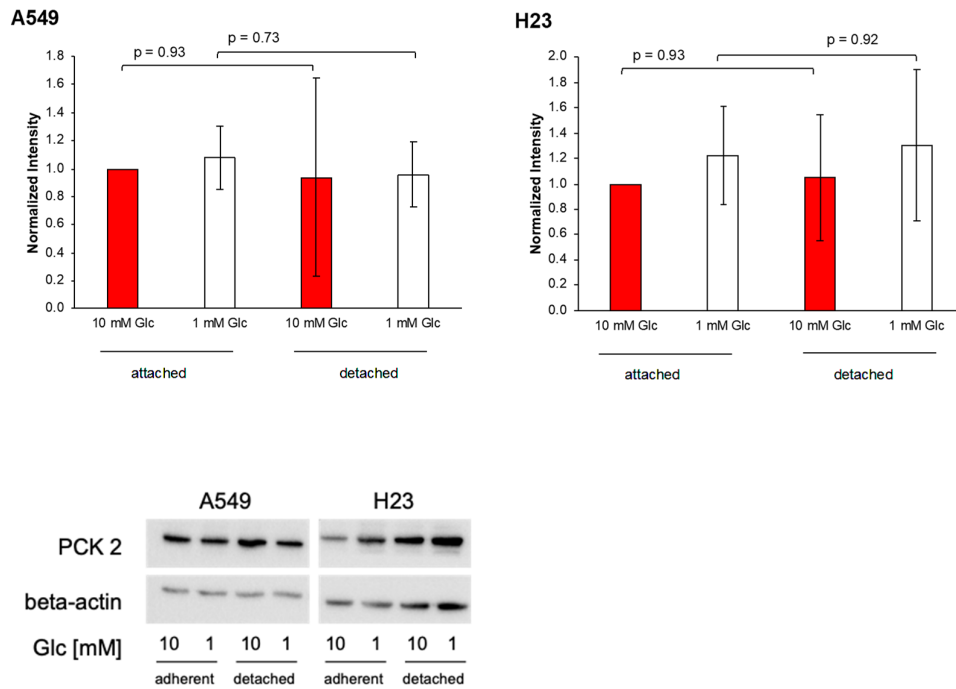


Figure 5: Western Blot of PCK2 expression in attached and detached A549 and H23 cells. Two glucose concentrations, 1 mM and 10 mM, supplemented with 10% dFCS were used to treat cells for 18 hours. Intensity values were normalized to high glucose and attached group for each cell line and then normalized to beta-actin. Data are mean \pm SEM from three independent experiments. Glc, glucose.

4.2.2 PCK2 RNA expression

In similar outcome to the Western blot results, RNA expression of PCK2 in A549 and H23 did not have any significant expression differences between attached and detached cells (**Figure 6**). Furthermore, serum or glucose starvation also did not significantly change the expression of PCK2 in both cell lines.

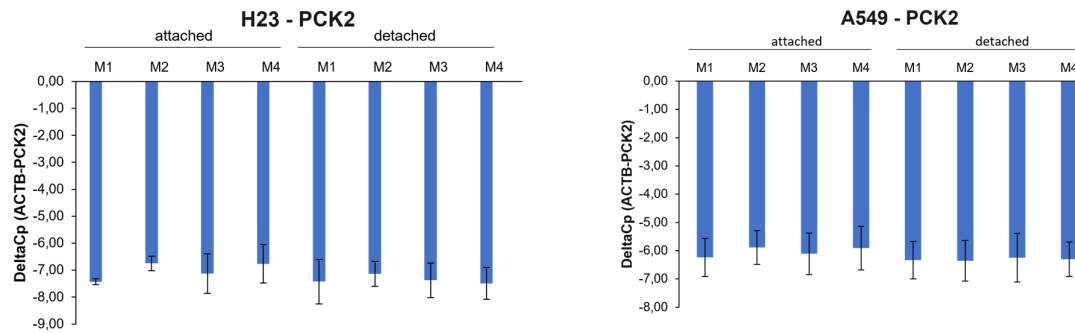


Figure 6: PCK2 RNA expression in attached and detached A549 and H23 cells: Cells were treated for 24 hours in media 1-4 (M1-M4). M1 = 10 mM glucose, 10 % dFCS, M2 = 10 mM glucose, 0 % dFCS, M3 = 1 mM glucose, 10 % dFCS, M4 = 1 mM glucose, 0 % dFCS. Data are mean \pm SEM from three independent experiments.

4.3 Confirmation of PCK2 silencing on mRNA level

In order to investigate the role of PCK2 in survival of H23 cancer cells under starvation and detachment, we silenced PCK2 using two different pools of PCK2 siRNA. First, we confirmed the efficacy of the siRNAs under our experimental conditions. We measured PCK2 RNA expression under all growth conditions in detached cells using qPCR. Both siRNAs significantly reduced PCK2 RNA levels (**Figure 7**). PCK2 siRNA 1 and PCK2 siRNA 2, were compared to control siRNA group (csi).

Media differences did not affect silencing on the RNA level. Additionally, we confirmed the efficacy of PCK2 siRNA treatment in conventionally cultured cells on the protein level by members of the Leithner group using Western blot (data not shown).

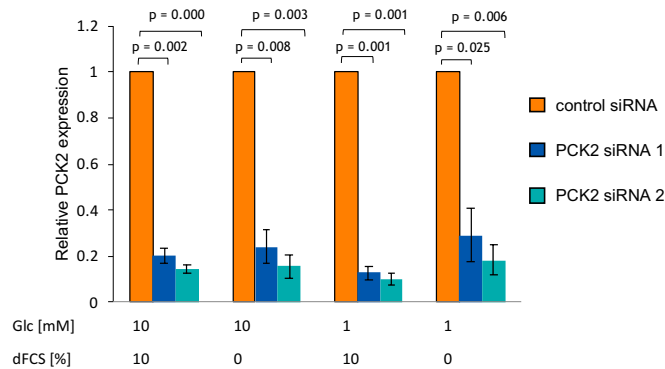


Figure 7: PCK2 expression analysis in H23 cells transfected with PCK2 siRNA and cultured in different growth media. Cells were transfected using two different pools of PCK2 siRNA, siRNA 1 and siRNA 2, or non-silencing siRNA (control siRNA). A, PCK2 mRNA levels in detached cells. Results were compared to control siRNA (csi) with one-group t-test. Data are mean \pm SEM from three independent experiments.

4.4 PCK2-silencing effects on viability and viable cell number

To test the influence of PCK2 on matrix-independent cell survival, H23 cells were transfected with the two different pools of siRNA silencing PCK2, as well as a control siRNA with non-targeting effects. Cell viability, and viable cell number of cells transfected with PCK siRNA 1 and PCK2 siRNA 2 were compared to control siRNA group. This analysis was done for each growth media group, to see if PCK2 silencing effects on cell survival depended on glucose concentrations and the presence of serum. First, results for medium containing high glucose (10 mM) and 10% dFCS are shown (**Figure 8**). Here, PCK2 silencing did not show any effect on cell viability. The viable cell number, interestingly, was significantly reduced by PCK2 siRNA 1 ($p = 0.0031$) and PCK2 siRNA 2 ($p = 0.041$).

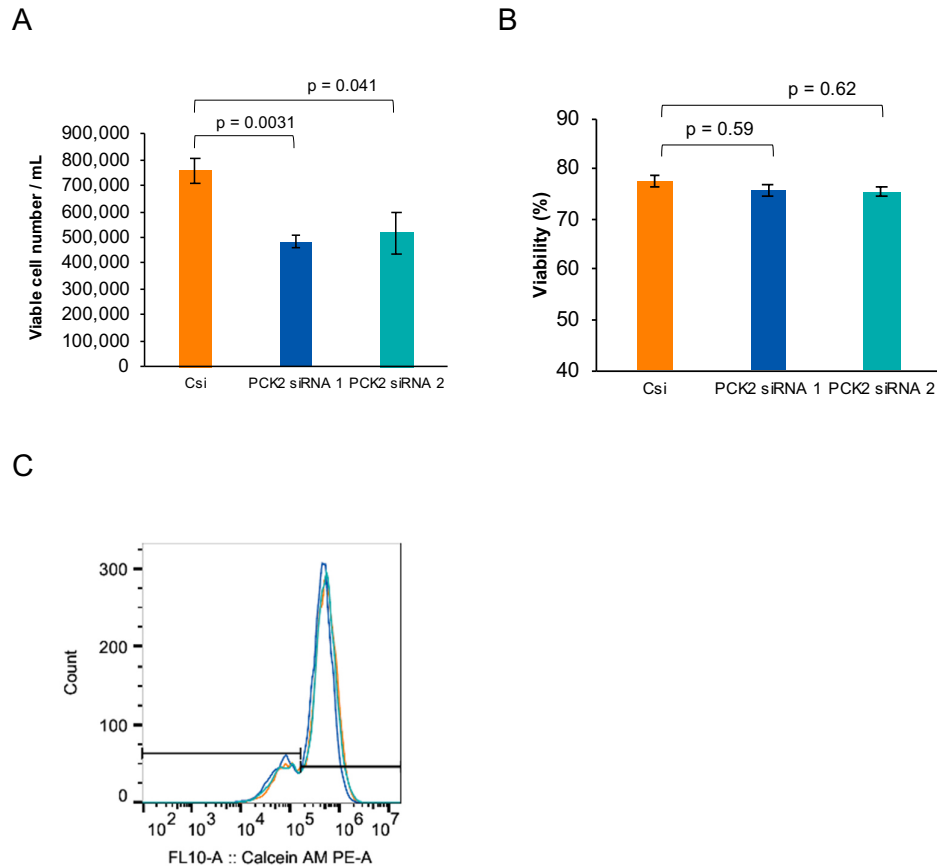


Figure 8: Cell numbers and viability of matrix-detached H23 cells - 10 mM glucose and 10% dFCS: Comparison of transfected H23 cells treated in high glucose with serum for 24 hours in ultra-low attachment plates. (A) Viable cell number of main transfection groups csi, PCK2 siRNA 1, PCK2 siRNA 2. (B) Cell viability of csi, PCK2 siRNA 1 and PCK2 siRNA 2, measured by FACS. (C) Histogram showing FACS fluorescence curves of main transfection groups, csi: orange, PCK2 siRNA 1: dark blue, PCK2 siRNA 2: teal. Results are shown as mean \pm SEM from four independent experiments.

Next, we compared cells cultured in 1 mM glucose and with 10% serum (**Figure 9**). PCK2 silencing did not have any significant impact on cell viability and viable cell number of cells treated in low glucose (1 mM) and with serum. However, viable cell numbers showed a decreasing trend in PCK2 siRNA 1 ($p = 0.17$) and PCK2 siRNA 2 ($p = 0.082$).

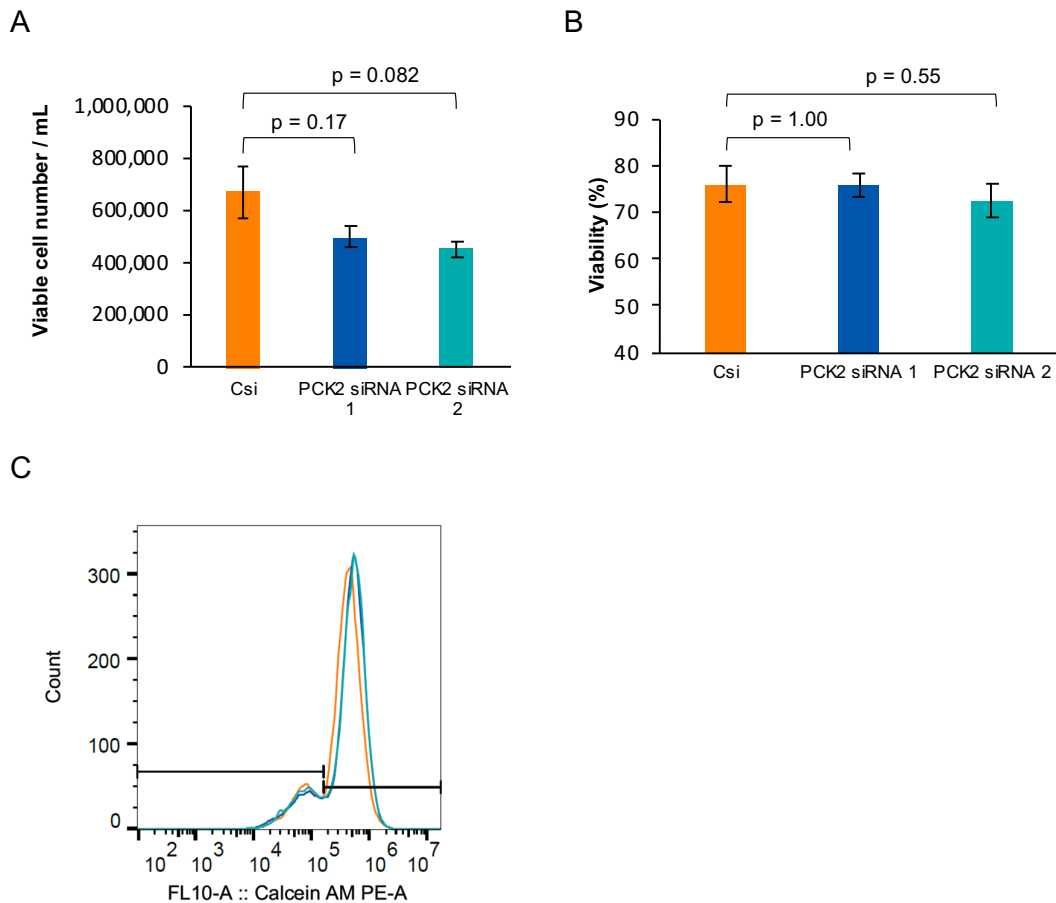


Figure 9: Cell numbers and viability of matrix-detached H23 cells - 1 mM glucose and 10% dFCS: Comparison of transfected H23 cells treated in low glucose with serum for 24 hours in ultra-low attachment plates. Results are shown as mean \pm SEM from four independent experiments. (A) Viable cell number of main transfection groups csi, PCK2 siRNA 1, PCK2 siRNA 2. (B) Cell viability of csi, PCK2 siRNA 1 and PCK2 siRNA#2. (C) Corresponding FACS fluorescence curves of main transfection groups, csi: orange, PCK2 siRNA 1: dark blue, PCK2 siRNA 2: teal. Results are shown as mean \pm SEM from four independent experiments.

Finally, we took a look at PCK2 silencing under conditions where cells lack serum completely. Cells treated in high glucose (10 mM) and without serum did not have significant differences in cell viability and viable cell number between control siRNA and PCK2 siRNA groups (**Figure 10**). Serum-free cells with low glucose treatment (1 mM) had significant differences in viable cell number of cells transfected with

PCK2 siRNA 1 ($p = 0.0045$) and showed a trend for PCK2 siRNA 2 ($p = 0.072$) (**Figure 11**). Cell viability under these conditions, showed a decreasing trend for PCK2 siRNA 2 ($p = 0.11$). As observed in our initial experiments, absolute viable cell numbers were very low in serum-free media compared to serum-containing media.

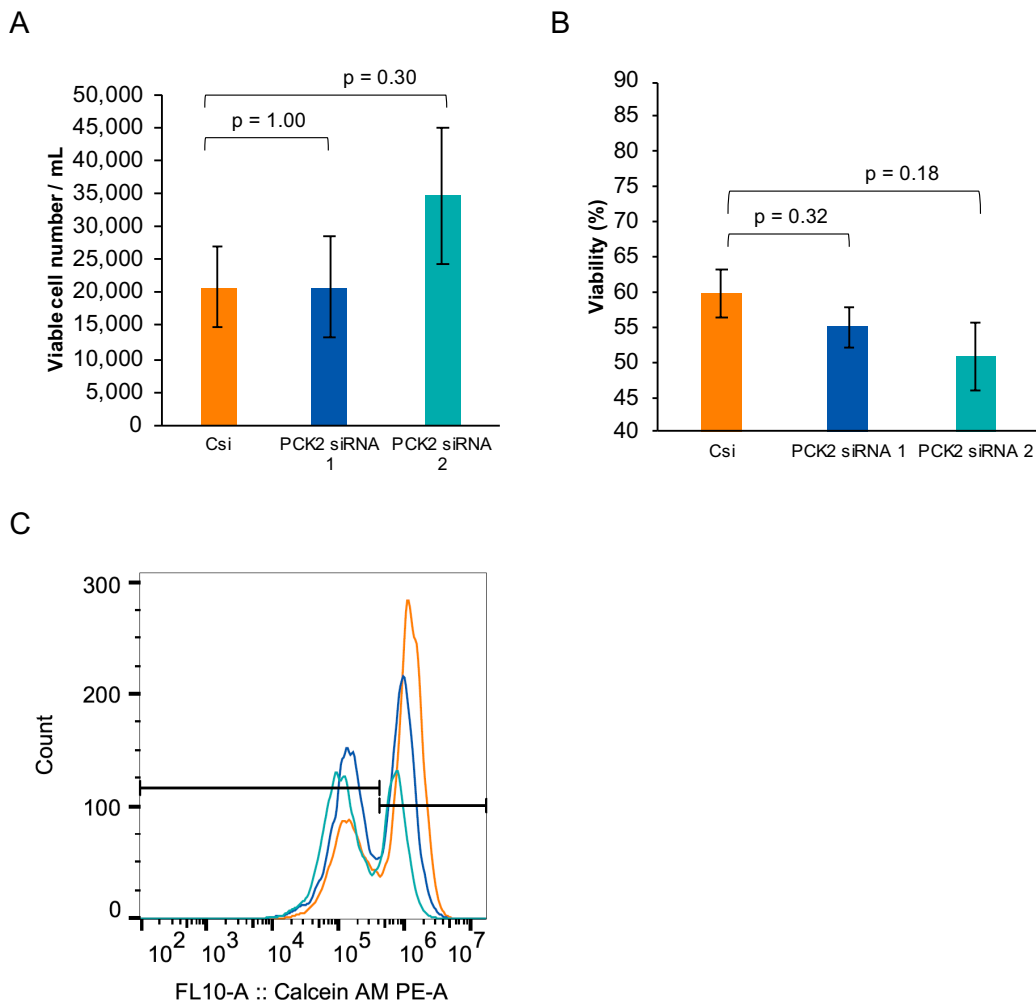


Figure 10: Cell numbers and viability of matrix-detached H23 cells - 10 mM glucose and 0% dFCS: Comparison of transfected H23 cells treated in high glucose without serum for 24 hours in ultra-low attachment plates. (A) Viable cell number of main transfection groups csi, PCK2 siRNA 1, fluorescence curves of main transfection groups, csi: orange, PCK2 siRNA 1: dark blue, PCK2 siRNA 2: teal. Results are shown as mean \pm SEM from four independent experiments.

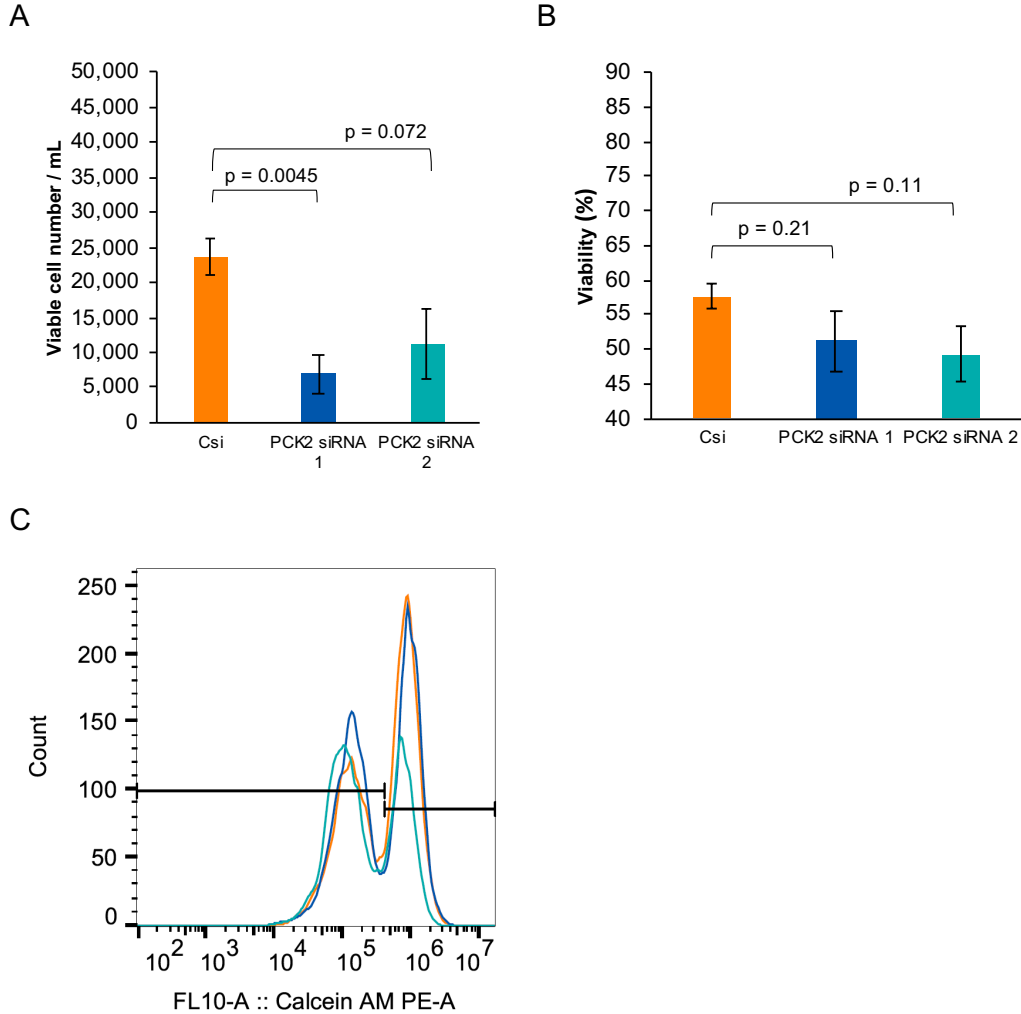


Figure 11: Cell numbers and viability of matrix-detached H23 cells - 1 mM glucose and 0% dFCS: Comparison of transfected H23 cells treated in low glucose without serum for 24 hours in ultra-low attachment plates. (A) Viable cell number of main transfection groups csi, PCK2 siRNA 1, PCK2 siRNA 2. (B) Cell viability of csi, PCK2 siRNA 1 and PCK2 siRNA#2. (C) Corresponding FACS fluorescence curves of main transfection groups, csi: orange, PCK2 siRNA 1: dark blue, PCK2 siRNA 2: teal. Results are shown as mean \pm SEM from four independent experiments.

4.5 Proliferation assay

The discrepancy between lower viable cell numbers under serum starvation compared to serum-containing medium as opposed to similar viability rates could be explained by differences in proliferation. While some cells underwent cell death, remaining cells potentially might have continued to proliferate in a serum-dependent manner. To investigate this potential factor, we performed a proliferation assay, of cells cultured in the same way as in cell viability and viable cell number experiments, using the EdU proliferation assay.

Obtained data was normalized to the 10 mM glucose 10% dFCS condition, due to a higher concentrated dye reaction mix in the first experiment, which led to higher values. All statistical analysis was then performed based on normalized values.

To test the proliferation assay, we included a negative control of detached cells that were not treated with EdU. The resulting FACS curve overlay of negative control and csi cells in 10 mM glucose and 10% dFCS shows a clear distinction between proliferating cells and non-proliferation cells (**Figure 12**).

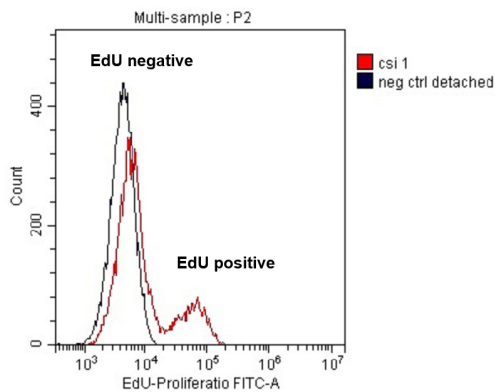


Figure 12: Quality control of proliferation assay –Cells were transfected with control siRNA (csi) in 10mM glucose and 10% dFCS and grown in detachment plates for 24 hours. Negative control (neg ctrl detached) did not receive EdU solution. Positive control shown in red (csi) is characterized

by two separate peaks, representing proliferating (EdU positive) and non-proliferating cells (Edu negative).

When we cultured H23 cells in ultra-low detachment plates exactly as for the viability and cell number assays, we found that cells treated without serum showed significantly lower proliferation than cells that received serum (**Figure 13**). This proved to be true for both, 10 mM glucose ($p = 0.05$) and 1 mM glucose ($p = 0.02$) conditions that lacked serum. This can be visually seen in FACS curves having lower proliferating peaks in cells lacking serum. Serum-starved cells had about 8 to 10 percentage points less proliferation than their counterpart.

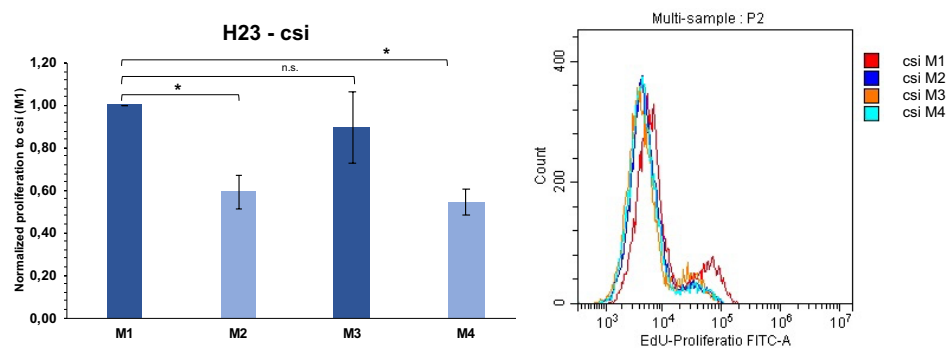


Figure 13: Effect of different media on proliferation in detached H23 cells transfected with control siRNA (csi) - Cells were treated for 24 hours in Media 1-4 (M1-M4). M1, 10 mM glucose, 10 % dFCS; M2, 10 mM glucose, 0 % dFCS; M3, 1 mM glucose, 10 % dFCS; M4, 1 mM glucose, 0 % dFCS. Proliferation was measured by detecting the incorporation of EdU followed by FACS analysis. Data are mean \pm SEM from three independent experiments. * $p < 0.05$.

PCK2 silencing with both PCK2 siRNA 1 and PCK2 siRNA 2 did not impact proliferation significantly in any of the tested media (**Figure 14**).

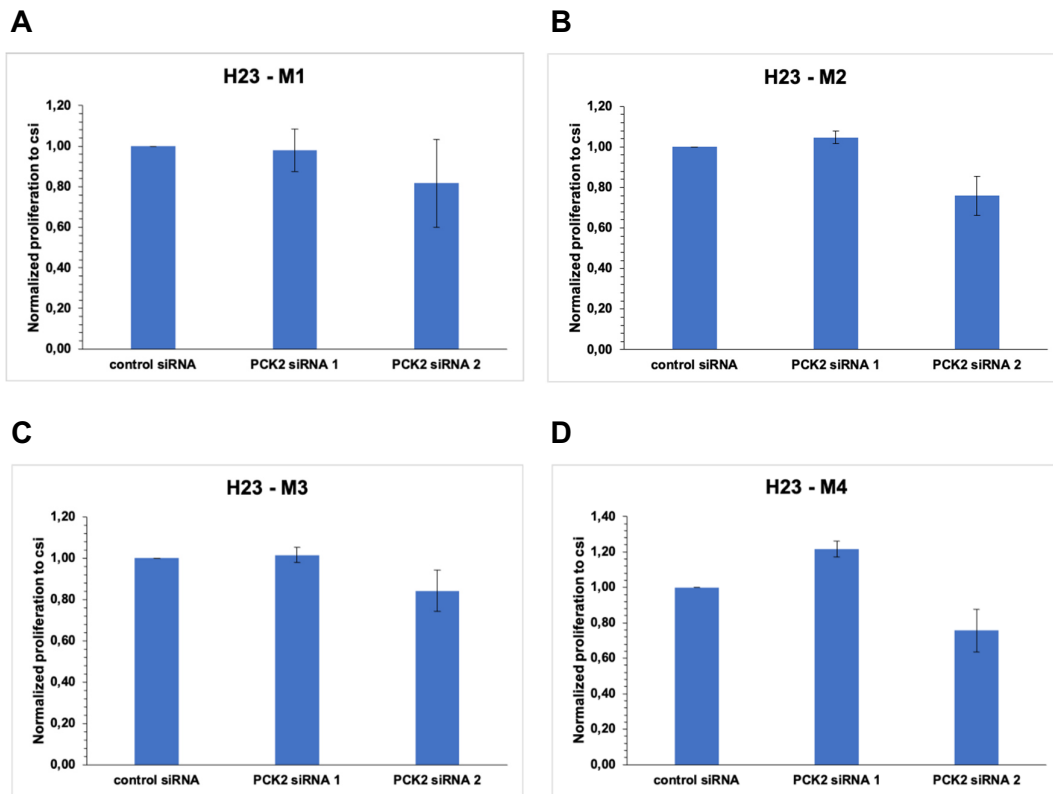


Figure 14: Effect of PCK2 silencing on proliferation in detached H23 cells in different media - Cells were treated for 24 hours in Media 1-4 (M1-M4). M1 = 10 mM glucose, 10 % dFCS, M2 = 10 mM glucose, 0 % dFCS, M3 = 1 mM glucose, 10 % dFCS, M4 = 1 mM glucose, 0 % dFCS. Data are mean \pm SEM from three independent experiments.

4.6 Gene expression analysis

To better understand how ECM detachment effects cells, we analyzed the expression of various genes linked with tumor growth, metabolism or survival.

4.6.1 Fatty acid synthase (FASN)

FASN mRNA was significantly upregulated in attached H23 cells under serum starvation compared to serum-containing medium in high glucose conditions ($p = 0.028$) (Figure 15). Moreover, a trend for increased expression of FASN in the absence of serum was found in low glucose medium This could suggest that in

absence of lipid-containing serum cells try to circumvent the lack of exogenous lipids, by increasing de-novo synthesis of fatty acids through FASN.

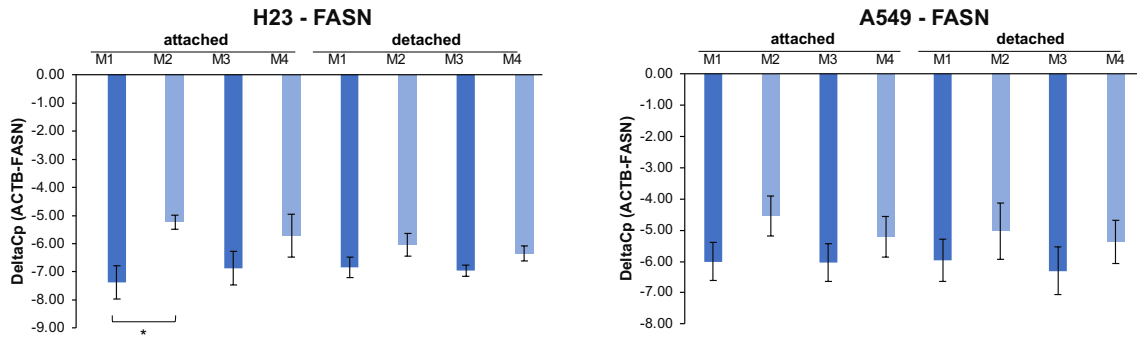


Figure 15: Fatty acid synthase (FASN) RNA expression in attached and detached A549 and H23 cells analyzed using qPCR: Cells were treated for 24 hours in Media 1-4 (M1-M4). M1, 10 mM glucose, 10 % dFCS; M2, 10 mM glucose, 0 % dFCS; M3, 1 mM glucose, 10 % dFCS; M4, 1 mM glucose, 0 % dFCS. Data are mean \pm SEM from three independent experiments. * $p < 0.05$.

4.6.2 GLUT-1 (SLC2A1)

Under serum starvation and isolation from the matrix, cells potentially increase their glucose uptake by upregulating the insulin-independent glucose transport protein GLUT-1 via overexpression of its gene SLC2A1. Therefore, we compared SLC2A1 gene expression between detached and attached cells, as well as between serum-free and serum-containing media (Figure 16). H23 and A549 cell lines did not show any significant overexpression of SLC2A1 under matrix-independency or absence of serum.

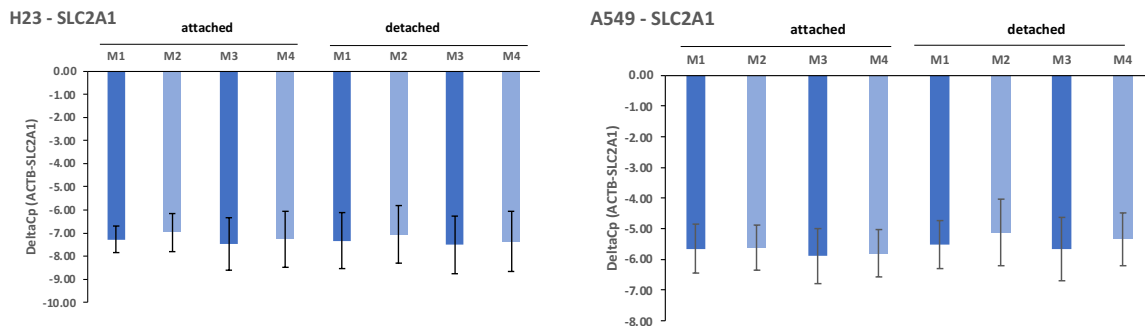


Figure 16: SLC2A1 mRNA expression in attached and detached A549 and H23 cells analyzed using qPCR: Cells were treated for 24 hours in Media 1-4 (M1-M4). M1, 10 mM glucose, 10 % dFCS; M2, 10 mM glucose, 0 % dFCS; M3, 1 mM glucose, 10 % dFCS; M4, 1 mM glucose, 0 % dFCS. Data are mean \pm SEM from three independent experiments.

4.6.3 Glutathione reductase (GSR)

Glutathione reductase, coded by the gene GSR, is an important enzyme for the regeneration of (reduced) glutathione. Glutathione is important for cells undergoing oxidative stress. Serum starvation or detachment from matrix can possibly present a triggering factor for oxidative stress (49).

The data obtained indicated that serum starvation and matrix-detachment did not trigger any significant overexpression of GSR in H23 and A549 cells. (**Figure 17**).

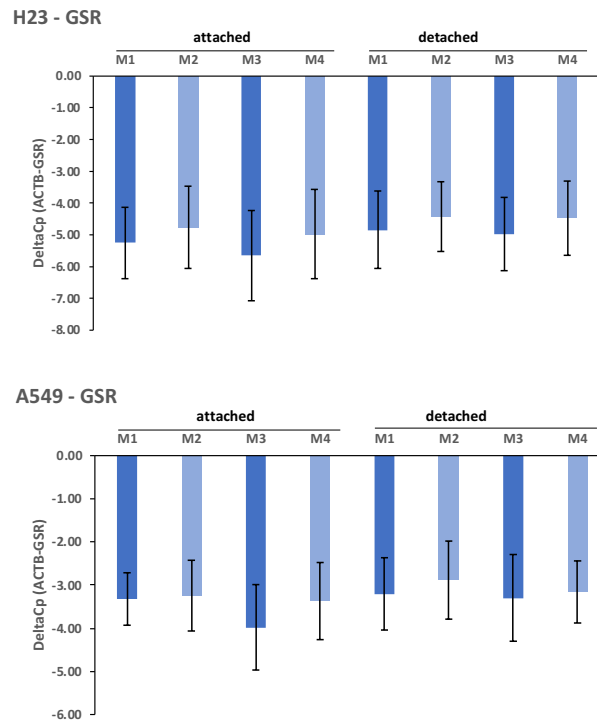


Figure 17: GSR mRNA expression in attached and detached A549 and H23 cells analyzed using qPCR: Cells were treated for 24 hours in Media 1-4 (M1-M4). M1, 10 mM glucose, 10 % dFCS; M2, 10 mM glucose, 0 % dFCS; M3, 1 mM glucose, 10 % dFCS; M4, 1 mM glucose, 0 % dFCS. Data are mean \pm SEM from three independent experiments.

4.6.4 Thioredoxin reductase 1 (TXNRD1)

The NADPH utilizing enzyme TXNRD1 is an alternative antioxidant enzyme. When we assessed expression levels of TXNRD1 we found no significant regulation by detachment or by the different nutritional conditions (**Figure 18**).

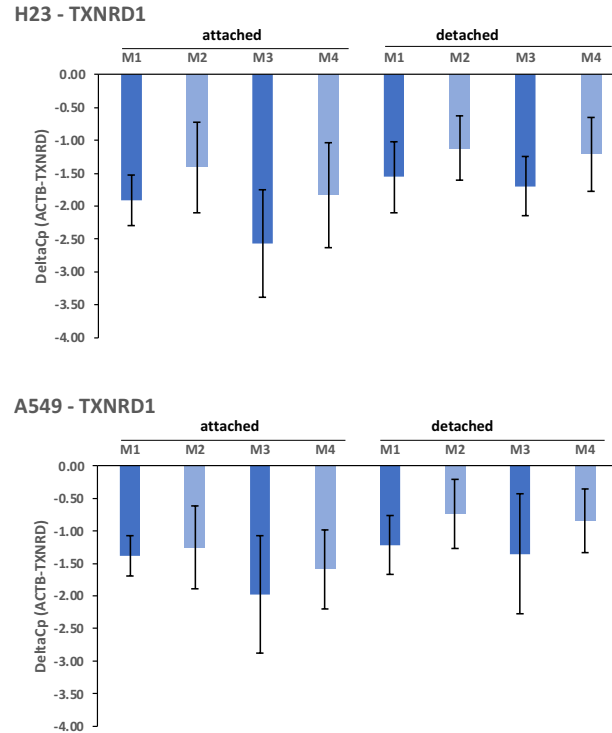


Figure 18: TXNRD1 mRNA expression in attached and detached H23 and A549 cells analyzed by qPCR: Cells were treated for 24 hours in Media 1-4 (M1-M4). M1, 10 mM glucose, 10 % dFCS; M2, 10 mM glucose, 0 % dFCS; M3, 1 mM glucose, 10 % dFCS; M4, 1 mM glucose, 0 % dFCS. Data are mean \pm SEM from three independent experiments.

5 Discussion

5.1 Interpretation of results

PCK2 already demonstrated significant effects on cell apoptosis in previous studies in attached cells under glucose deprivation (24). Our aim was to investigate how susceptible PCK2 silenced matrix-detached NSCLC cells were to poor metabolic conditions. In reference to our hypothesis, the results suggest that PCK2 has impact on overall cell survival in ECM detached cells. Significant viable cell number differences were observed in high glucose media with serum and in low glucose without serum. Matrix independency did not induce overexpression of PCK2 on both the protein and mRNA level, suggesting that PCK2 expression is not affected by ECM attachment in H23 NSCLC cells. In this setting, glucose concentration and serum availability could both not be clearly isolated as associated variables in the effect of PCK2 on cell survival.

In general, the presence of serum, could be identified to have impact on cell survival and viability under ECM detachment. Reduced proliferation under serum starvation could explain the relatively low viable cell numbers measured. Also, rapid cell death could have led to an overestimation of cell viability. It remains unclear how early or fast cell death took place, so cell viability has to be interpreted cautiously.

5.2 PCK2 demand due to raised FASN levels?

FASN is able to use carbohydrates and convert them into fatty acids and is commonly upregulated in various tumors. In gene expression analysis we found raised FASN mRNA levels under serum starvation and high glucose in attached H23 cells. Serum starvation might have initiated some form of metabolic reprogramming by upregulating the endogenous biosynthesis of lipids. It could suggest that the gluconeogenic enzyme PCK2 supports this lipid demand in cancer cells, as it occurs physiologically in hepatocytes and adipocytes (17). However, the reverse pathway of glycolysis has also to be considered as possible provider of glycerin, especially

when glucose is abundant. It is important to note that it remains unclear how lipid and glycerin synthesis is actually affected and to what degree the increased FASN mRNA levels translate to in actual protein expression. The hypothesis of PCK2 aiding in glyceroneogenesis could in part explain the effect of PCK2 silencing on cell survival in the low glucose and serum-free environment.

5.3 Serum may contain necessary growth and survival factors

Serum supplementation is routinely used in cell culture. In our experimental conditions, the availability of dialyzed fetal calf serum had major implications on cell survival and proliferation. The dialysis process reduced the concentration of small molecules like amino acids, hormones and cytokines, but retained macromolecules present in FCS. It is known that serum contains a multitude of proteins, some of which confer growth under anchorage independent growth conditions, but also lipids, which may be used as nutrients. In-vivo studies using Lewis lung cancer cells identified fetuin A to be one such responsible growth factor (54). Further, serum exosomes, small vesicles that can contain nucleic acids or small proteins, have also been found to be associated with anchorage independent growth (55). Growth factor signaling derived from serum-containing media could be of equal importance for our NSCLC cells and explain the declines in survival and proliferation we observed.

5.4 Influence of glucose concentrations

Glucose concentration of 1 mM did not show any effects on cell viability and survival in our NSCLC cells compared to a high-normal concentration of 10 mM. Cell line specific oncogenic mutations could have rescued glucose uptake in our detached NSCLC cells, similarly to ERBB2 expressing mammary epithelial cells (49). NSCLC cells in attachment to the ECM have already been tested in previous studies by members our study group (24) and cells were able to adapt to concentrations of 1 mM glucose. When glucose was lowered to 0.2 mM, PCK2 silencing significantly induced apoptosis. In conclusion, a concentration of 1 mM was not low enough to induce significant PCK2 expression in detached cells and cell survival was similar

in 1 and 10 mM glucose. This suggests that cancer cells readily adapt to a 10-fold decrease of glucose, also under detachment. Unpublished data from the Leithner group suggest that at 1 mM glucose, glycolysis and lactate production are still maintained in attached lung cancer cells, possibly due to highly efficient glucose transport and trapping in the cancer cells.

5.5 Limitations

Experiments were performed in a set of four or three independent runs. Some results suggest a trend and might show statistical significance, if more experimental runs would have been included. In this study, cell viability and proliferation as cell survival and growth parameters were assessed. A potentially important factor to consider is the appropriate choice of treatment time. The selected 24-hour treatment time might be too short. Several measuring time points could give impression of the survival course over time and differences might become more prominent after longer treatment times. We only used H23 cells in PCK2 experiments, so cell line specific interactions could be present. A549 cell were also tried in early groundwork of PCK2 silencing experiments, but due to poor survival under low-attachment conditions this cell-line was omitted from further analysis. Inclusion of more NSCLC cell lines could rule out or identify any cell line specific differences.

5.6 Outlook

In future, treatments targeting the function of PCK2 could potentially be exploited and possibly enhance the currently poor treatment options for NSCLC patients. A synthetically synthesized compound, iPEPCK2, has already been successfully tested in epithelial and colon carcinoma cells, as well as in murine xenograft models (56). Still, there is still a lot of missing data on how PCK2 actually affects tumors under different metabolic conditions. Moreover, detailed analyses of cancer cells metabolism e.g. using stable isotopic tracers in cancer cells with or without matrix detachment are needed.

In terms of our experimental setting, we only assessed cell viability as in the fraction of living cells under in-vitro conditions. Measuring apoptosis in suitable apoptosis assays could shed more light on to specific cell death analysis. Since serum components were identified to have big impact on detached cells one could investigate the possible effect of serum exosomes and lipids in fetal calf serum. If serum exosomes are of importance for growth and survival, they could be extracted and purified to be used to optimize serum-free media.

5.7 Conclusion

We established an experimental setting to test PCK2 effects in matrix-detached NSCLC cells under various metabolic conditions. Although detachment from the ECM did not induce PCK2 overexpression, data suggests that PCK2 silencing affected matrix detached cell survival. Glucose and serum availability could not be clearly identified as determining variable in the effect of PCK2 silencing. Strikingly, serum-free media impaired viable cell number and proliferation in our in-vitro detachment model. Therefore, possible side factors in serum, like exosomes and lipids, should be tested in future. Further research will be required to elucidate the role of PCK2 in matrix independent NSCLC cells and metastasis.

6 References

1. Adler IA. Primary Malignant Growths of the Lung. CA: A Cancer Journal for Clinicians. 1980;30(5):295–301.
2. GLOBOCAN. Number of new cases in 2020, both sexes, all ages. World Health Organization. 2020.
3. Wynder EL. Tobacco as a cause of lung, cancer: Some reflections. Vol. 146, American Journal of Epidemiology. Oxford University Press; 1997. p. 687–94.
4. Doll R, Peto R, Boreham J, Sutherland I. Mortality in relation to smoking: 50 Years' observations on male British doctors. British Medical Journal. 2004;328(7455):1519–28.
5. Hecht SS. Tobacco carcinogens, their biomarkers and tobacco-induced cancer. Vol. 3, Nature Reviews Cancer. European Association for Cardio-Thoracic Surgery; 2003. p. 733–44.
6. Sun S, Schiller JH, Gazdar AF. Lung cancer in never smokers - A different disease. Vol. 7, Nature Reviews Cancer. Nature Publishing Group; 2007. p. 778–90.
7. Böcker W, Denk H, Heitz PU. Pathologie. 5th ed. Elsevier Urban&Fischer; 2012. 1064 p.
8. Goldstraw P, Crowley J, Chansky K, Giroux DJ, Groome PA, Rami-Porta R, et al. The IASLC Lung Cancer Staging Project: Proposals for the Revision of the TNM Stage Groupings in the Forthcoming (Seventh) Edition of the TNM Classification of Malignant Tumours. Journal of Thoracic Oncology. 2007;2(8):706–14.
9. Arbour KC, Riely GJ. Systemic therapy for locally advanced and metastatic non-small cell lung cancer: A review. JAMA - Journal of the American Medical Association. 2019;322(8):764–74.
10. Warburg O. The metabolism of carcinoma cells 1. The Journal of Cancer Research. 1925;9(1):148–63.
11. Shestov AA, Liu X, Ser Z, Cluntun AA, Hung YP, Huang L, et al. Quantitative determinants of aerobic glycolysis identify flux through the enzyme GAPDH as a limiting step. eLife. 2014 ;3(2014):1–18.
12. Pfeiffer T, Schuster S, Bonhoeffer S. Cooperation and competition in the evolution of ATP-producing pathways. Science. 2001;292(5516):504–7.
13. Heiden MG, Cantley LC, Thompson CB. Understanding the warburg effect: The metabolic requirements of cell proliferation. Vol. 324, Science. American Association for the Advancement of Science; 2009. p. 1029–33.
14. Horn F. Biochemie des Menschen. 8th ed. Stuttgart, Germany: Thieme; 2020.
15. Grasmann G, Smolle E, Olschewski H, Leithner K. Gluconeogenesis in cancer

- cells – Repurposing of a starvation-induced metabolic pathway? Vol. 1872, *Biochimica et Biophysica Acta - Reviews on Cancer*. *Biochim Biophys Acta Rev Cancer*; 2019. p. 24–36.
16. Hanson RW, Patel YM. Phosphoenolpyruvate Carboxykinase (GTP): The Gene and the Enzyme. *Advances in Enzymology and Related Areas of Molecular Biology*. 2006;69:203–81.
 17. Hanson RW, Reshef L. Glyceroneogenesis revisited. In: *Biochimie*. Elsevier; 2003. p. 1199–205.
 18. Owen OE, Kalhan SC, Hanson RW. The Key Role of Anaplerosis and Cataplerosis for Citric Acid Cycle Function *. *Journal of Biological Chemistry*. 2002;277(34):30409–12.
 19. Martin JD, Fukumura D, Duda DG, Boucher Y, Jain RK. Reengineering the Tumor Microenvironment to Alleviate Hypoxia and Overcome Cancer Heterogeneity. *Cold Spring Harbor Perspectives in Medicine*. 2016;6(12):a027094.
 20. Vaupel P. Tumor microenvironmental physiology and its implications for radiation oncology. *Seminars in Radiation Oncology*. 2004;14(3):198–206.
 21. Sullivan MR, Danai L V., Lewis CA, Chan SH, Gui DY, Kunchok T, et al. Quantification of microenvironmental metabolites in murine cancers reveals determinants of tumor nutrient availability. *eLife*. 2019;8.
 22. Ziaian B, Saberi A, Ghayyoumi MA, Safaei A, Ghaderi A, Mojtahedi Z. Association of high LDH and low glucose levels in pleural space with HER2 expression in non-small cell lung cancer. *Asian Pacific Journal of Cancer Prevention*. 2014;15(4):1617–20.
 23. Brooks GA. The Science and Translation of Lactate Shuttle Theory. *Cell Metabolism*. 2018;27(4):757–85.
 24. Leithner K, Hrzenjak A, Trötz Müller M, Moustafa T, Köfeler HC, Wohlkoenig C, et al. PCK2 activation mediates an adaptive response to glucose depletion in lung cancer. *Oncogene* 2015 34:8. 2014;34(8):1044–50.
 25. Pavlova NN, Thompson CB. The Emerging Hallmarks of Cancer Metabolism. Vol. 23, *Cell Metabolism*. Cell Press; 2016. p. 27–47.
 26. Vander Heiden MG, DeBerardinis RJ. Understanding the Intersections between Metabolism and Cancer Biology. *Cell*. 2017;168(4):657–69.
 27. Hosios AM, Hecht VC, Danai L V., Johnson MO, Rathmell JC, Steinhauser ML, et al. Amino Acids Rather than Glucose Account for the Majority of Cell Mass in Proliferating Mammalian Cells. *Developmental Cell*. 2016;36(5):540–9.
 28. DeBerardinis RJ, Chandel NS. Fundamentals of cancer metabolism. *Science Advances*. 2016;2(5):e1600200.
 29. Davidson SM, Papagiannakopoulos T, Olenchock BA, Heyman JE, Keibler

- MA, Luengo A, et al. Environment Impacts the Metabolic Dependencies of Ras-Driven Non-Small Cell Lung Cancer. *Cell Metabolism*. 2016;23(3):517–28.
30. Hensley CT, Wasti AT, DeBerardinis RJ. Glutamine and cancer: cell biology, physiology, and clinical opportunities. *The Journal of Clinical Investigation*. 2013;123(9):3678–84.
 31. Sellers K, Fox MP, li MB, Slone SP, Higashi RM, Miller DM, et al. Pyruvate carboxylase is critical for non-small-cell lung cancer proliferation. *Journal of Clinical Investigation*. 2015;125(2):687–98.
 32. Muir A, Danai L V., Gui DY, Waingarten CY, Lewis CA, Vander Heiden MG. Environmental cystine drives glutamine anaplerosis and sensitizes cancer cells to glutaminase inhibition. *eLife*. 2017;6.
 33. Gao Y, Wang X, Sang Z, Li Z, Liu F, Mao J, et al. Quantitative proteomics by SWATH-MS reveals sophisticated metabolic reprogramming in hepatocellular carcinoma tissues. *Scientific Reports* 2017 7:1. 2017;7(1):1–12.
 34. Sanders E, Diehl S. Analysis and interpretation of transcriptomic data obtained from extended Warburg effect genes in patients with clear cell renal cell carcinoma. *Oncoscience*. 2015;2(2):151–86.
 35. Xu D, Wang Z, Xia Y, Shao F, Xia W, Wei Y, et al. The gluconeogenic enzyme PCK1 phosphorylates INSIG1/2 for lipogenesis. *Nature*. 2020;580(7804):530–5.
 36. Smolle E, Leko P, Stacher-Priehse E, Brcic L, El-Heliebi A, Hofmann L, et al. Distribution and prognostic significance of gluconeogenesis and glycolysis in lung cancer. *Molecular Oncology*. 2020;14(11):2853–67.
 37. Leithner K, Triebel A, Trötz Müller M, Hinteregger B, Leko P, Wieser BI, et al. The glycerol backbone of phospholipids derives from noncarbohydrate precursors in starved lung cancer cells. *Proceedings of the National Academy of Sciences of the United States of America*. 2018;115(24):6225–30.
 38. Vincent EE, Sergushichev A, Griss T, Gingras MC, Samborska B, Ntimbane T, et al. Mitochondrial Phosphoenolpyruvate Carboxykinase Regulates Metabolic Adaptation and Enables Glucose-Independent Tumor Growth. *Molecular Cell*. 2015;60(2):195–207.
 39. Keshet R, Lee JS, Adler L, Iraqi M, Ariav Y, Lim LQJ, et al. Targeting purine synthesis in ASS1-expressing tumors enhances the response to immune checkpoint inhibitors. *Nature Cancer* 2020 1:9. 2020;1(9):894–908.
 40. Chen J, Lee HJ, Wu X, Huo L, Kim SJ, Xu L, et al. Gain of glucose-independent growth upon metastasis of breast cancer cells to the brain. *Cancer Research*. 2015;75(3):554–65.
 41. Montal ED, Dewi R, Bhalla K, Ou L, Hwang BJ, Ropell AE, et al. PEPCK Coordinates the Regulation of Central Carbon Metabolism to Promote Cancer

- Cell Growth. *Molecular Cell*. 2015;60(4):571–83.
42. Zhao J, Li J, Fan TWM, Hou SX. Glycolytic reprogramming through PCK2 regulates tumor initiation of prostate cancer cells. *Oncotarget*. 2017;8(48):83602.
 43. Bluemel G, Planque M, Madreiter-Sokolowski CT, Haitzmann T, Hrzenjak A, Graier WF, et al. PCK2 opposes mitochondrial respiration and maintains the redox balance in starved lung cancer cells. *Free Radical Biology and Medicine*. 2021;176:34–45.
 44. Moreno-Felici J, Hyroššová P, Aragó M, Rodríguez-Arévalo S, García-Rovés PM, Escolano C, et al. Phosphoenolpyruvate from Glycolysis and PEPCCK Regulate Cancer Cell Fate by Altering Cytosolic Ca²⁺. *Cells* 2020, Vol 9, Page 18. 2019;9(1):18.
 45. Frisch SM, Screaton RA. Anoikis mechanisms. *Current Opinion in Cell Biology*. 2001;13(5):555–62.
 46. Aceto N, Bardia A, Miyamoto DT, Donaldson MC, Wittner BS, Spencer JA, et al. Circulating Tumor Cell Clusters Are Oligoclonal Precursors of Breast Cancer Metastasis. *Cell*. 2014;158(5):1110–22.
 47. Fung C, Lock R, Gao S, Salas E, Debnath J. Induction of autophagy during extracellular matrix detachment promotes cell survival. *Molecular Biology of the Cell*. 2008;19(3):797–806.
 48. Mathew R, Karantza-Wadsworth V, White E. Role of autophagy in cancer. Vol. 7, *Nature Reviews Cancer*. *Nat Rev Cancer*; 2007. p. 961–7.
 49. Schafer ZT, Grassian AR, Song L, Jiang Z, Gerhart-Hines Z, Irie HY, et al. Antioxidant and oncogene rescue of metabolic defects caused by loss of matrix attachment. *Nature* 2009 461:7260. 2009;461(7260):109–13.
 50. Brown CW, Amante JJ, Goel HL, Mercurio AM. The $\alpha 6\beta 4$ integrin promotes resistance to ferroptosis. *Journal of Cell Biology*. 2017;216(12):4287–97.
 51. Brown CW, Amante JJ, Mercurio AM. Cell clustering mediated by the adhesion protein PVRL4 is necessary for $\alpha 6\beta 4$ integrin–promoted ferroptosis resistance in matrix-detached cells. *Journal of Biological Chemistry*. 2018;293(33):12741–8.
 52. Brieger K, Schiavone S, Miller FJ, Krause KH. Reactive oxygen species: From health to disease. Vol. 142, *Swiss Medical Weekly*. EMH Media; 2012.
 53. Boada J, Roig T, Perez X, Gamez A, Bartrons R, Cascante M, et al. Cells overexpressing fructose-2,6-bisphosphatase showed enhanced pentose phosphate pathway flux and resistance to oxidative stress. *FEBS Letters*. 2000;480(2–3):261–4.
 54. Kundranda MN, Henderson M, Carter KJ, Gorden L, Binhazim A, Ray S, et al. The Serum Glycoprotein Fetuin-A Promotes Lewis Lung Carcinoma Tumorigenesis via Adhesive-Dependent and Adhesive-Independent

Mechanisms. *Cancer Research*. 2005;65(2):499 LP – 506.

55. Ochieng J, Pratap S, Khatua AK, Sakwe. AM. Anchorage Independent Growth of Breast Carcinoma Cells is Mediated by Serum Exosomes. *Experimental cell research*. 2009 ;315(11):1875.
56. Aragón M, Moreno-Felici J, Abás S, Rodríguez-Arévalo S, Hyroššová P, Figueras A, et al. Pharmacology and preclinical validation of a novel anticancer compound targeting PEPCK-M. *Biomedicine and Pharmacotherapy*. 2020;121(October 2019).